

# Nanofabrication

**Nanofabrication** is the process of making functional structures with arbitrary patterns having minimum dimension currently defined to be  $\leq 100$  nm.

**motivation:** increase the density of components  
 lower their cost  
 increase their performance per device/integrated circuit

THE INTERNATIONAL TECHNOLOGY ROADMAP FOR SEMICONDUCTORS: 2010 UPDATE  
[www.itrs.net](http://www.itrs.net)

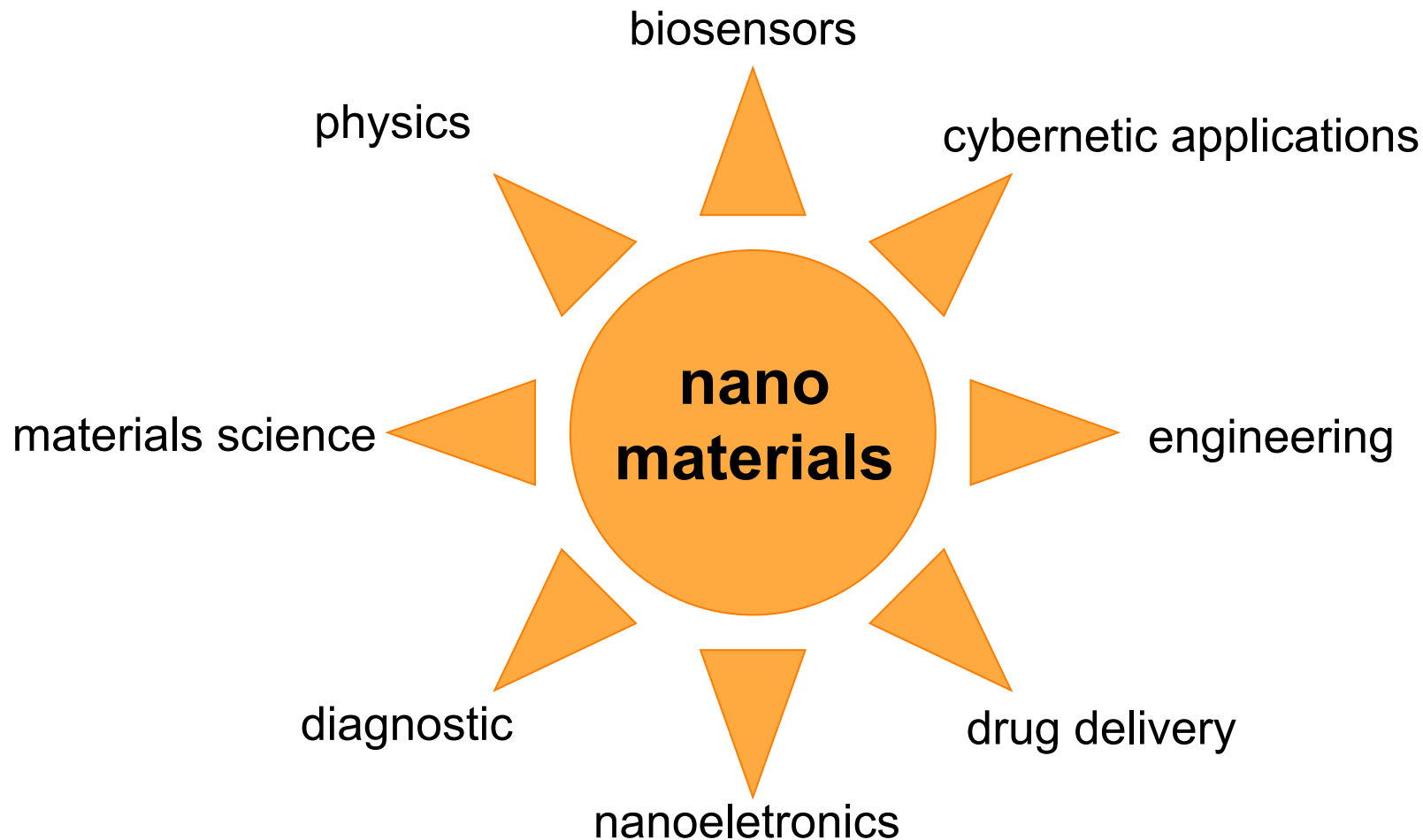
- In 2010, Flash devices are being manufactured using 32 nm half-pitch double patterning (DP)
- Current half-pitch of manufactured dynamic random-access memory (DRAM) is 40 nm.

| Year of Production                              | 2009 | 2010 | 2011 | 2012 | 2013 | 2014 | 2015 | 2016 | 2017 | 2018 | 2019  | 2020  | 2021  | 2022  | 2023  | 2024  |
|---|------|------|------|------|------|------|------|------|------|------|-------|-------|-------|-------|-------|-------|
| DRAM 1/2 pitch (nm) (contacted)                 | 52   | 45   | 40   | 36   | 32   | 28   | 25   | 23   | 20   | 18   | 16    | 14    | 13    | 11    | 10    | 9     |
| DRAM/Flash CD control (3 sigma) (nm)            | 5.4  | 4.7  | 4.2  | 3.7  | 3.3  | 2.9  | 2.6  | 2.3  | 2.1  | 1.9  | 1.7   | 1.5   | 1.3   | 1.2   | 1.0   | 0.9   |
| MPU/ASIC Metal 1 (M1) 1/2 pitch (nm)(contacted) | 54   | 45   | 38   | 32   | 27   | 24   | 21   | 19   | 17   | 15   | 13    | 12    | 11    | 9     | 8     | 8     |
| MPU gate in resist (nm)                         | 47   | 41   | 35   | 31   | 28   | 25   | 22   | 20   | 18   | 16   | 14    | 12    | 11    | 10    | 9     | 8     |
| MPU physical gate length (nm)                   | 29   | 27   | 24   | 22   | 20   | 18   | 17   | 15   | 14   | 13   | 12    | 11    | 10    | 9     | 8     | 7     |
| Gate CD control (3 sigma) (nm) [B]              | 3.0  | 2.8  | 2.5  | 2.3  | 2.1  | 1.9  | 1.7  | 1.6  | 1.5  | 1.3  | 1.2   | 1.1   | 1.0   | 0.9   | 0.8   | 0.8   |
| Overlay (3 sigma) (nm)                          | 10.3 | 9.0  | 8.0  | 7.1  | 6.4  | 5.7  | 5.1  | 4.5  | 4.0  | 3.6  | 3.2   | 2.8   | 2.5   | 2.3   | 2.0   | 1.8   |
| Contact after etch (nm)                         | 60   | 51   | 43   | 36   | 30   | 27   | 24   | 21   | 19   | 17   | 15    | 13    | 12    | 11    | 9     | 8     |
| Data Volume (GB)                                | 328  | 413  | 520  | 655  | 826  | 1040 | 1311 | 1651 | 2080 | 2621 | 3302  | 4161  | 5242  | 6605  | 8321  | 10484 |
| Grid Size (nm)                                  | 0.5  | 0.25 | 0.25 | 0.25 | 0.25 | 0.25 | 0.25 | 0.25 | 0.25 | 0.25 | 0.125 | 0.125 | 0.125 | 0.125 | 0.125 | 0.125 |

Manufacturable solutions exist, and are being optimized  
 Manufacturable solutions are known  
 Interim solutions are known  
 Manufacturable solutions are NOT known



## design, creation and characterization of nanostructures and nanostructured materials



## ■ conventional techniques for nanofabrication

- Photolithography
- Scanning Beam Litography

## ■ unconventional techniques

- nanofabrication by molding and embossing
- nanofabrication by printing
- scanning probe lithography
- edge lithography
- self-assembly for nanofabrication

**Table 1. Capabilities of Conventional and Unconventional Nanofabrication Techniques**

| technique   | current capabilities (2004)  |            |  |
|---|------------------------------|------------|--|
|   | minimum feature <sup>a</sup> | resolution | pattern  |
| photolithography <sup>1,b</sup>                           | 37 nm                        | 90 nm      | parallel generation of arbitrary patterns          |
| scanning beam lithography <sup>88,c</sup>                 | 5 nm                         | 20 nm      | serial writing of arbitrary patterns               |
| molding, embossing, and printing <sup>116,123,168,d</sup> | ~5 nm                        | 30 nm      | parallel formation of arbitrary patterns           |
| scanning probe lithography <sup>28,52</sup>               | <1 nm                        | 1 nm       | serial positioning of atoms in arbitrary patterns  |
| edge lithography <sup>39,e</sup>                          | 8 nm                         | 16 nm      | parallel generation of noncrossing features        |
| self-assembly <sup>353-357,f</sup>                        | >1 nm                        | >1 nm      | parallel assembly of regular, repeating structures |

<sup>a</sup> Refers to the minimum demonstrated lateral dimension. <sup>b</sup> A resolution (pitch) of 45 nm is projected for 2010 using 157-nm light, soft X-rays, or optical “tricks” (e.g., immersion optics). <sup>c</sup> Obtained with a focused ion beam. Limited by photoresist sensitivity and beam intensity. <sup>d</sup> Limited by available masters and, ultimately, van der Waals interactions. <sup>e</sup> Potentially smaller sizes could be obtained using atomic layer deposition. <sup>f</sup> Self-assembly produces structures with critical feature sizes from 1 to 100 nm or larger.

C. G. Willson, G. M. Whitesides *et al.* *Chem. Rev.* **2005**, *105*, 1171.

TABLE 1.1. Comparison of primary nanolithography techniques. Note that all numbers quoted are approximate and highly configuration/application dependent

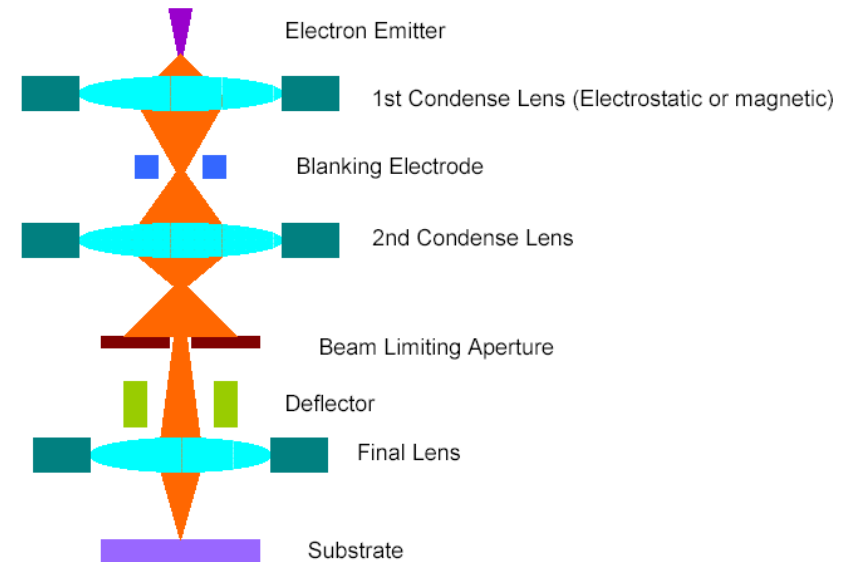
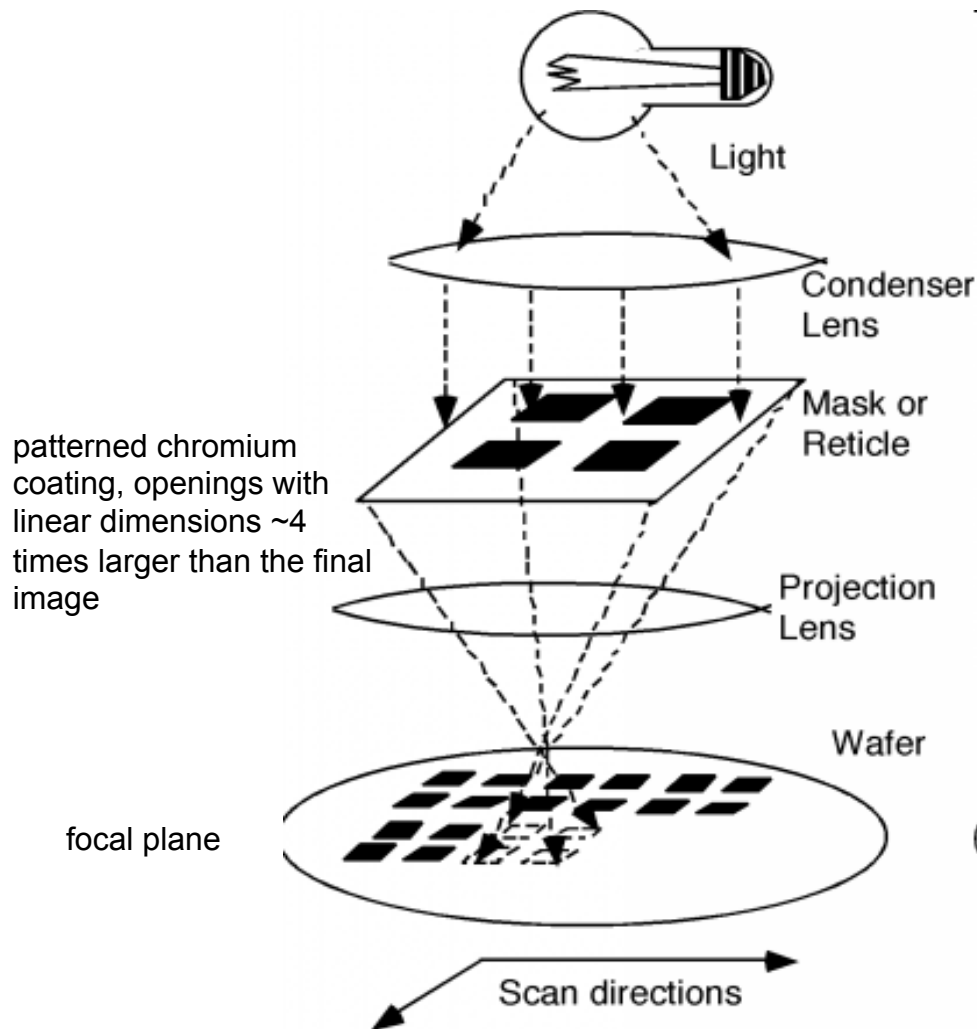
| Technique                           | Optical          | E-Beam<br>(Direct Write) | E-Beam<br>(Projection) | Focused<br>Ion Beam              | EUV                   | Nano-<br>Imprint |
|-------------------------------------|------------------|--------------------------|------------------------|----------------------------------|-----------------------|------------------|
| Resolution (nm)                     | 100              | 20                       | 50                     | 30                               | 30                    | 10               |
| Alignment (nm) <sup>a</sup>         | 30               | 10                       | 20                     | 10                               | 10                    | 100              |
| Throughput (Feature/s) <sup>b</sup> | 10 <sup>10</sup> | 10 <sup>4</sup>          | 10 <sup>10</sup>       | 10 <sup>1</sup> –10 <sup>2</sup> | 10 <sup>11</sup>      | 10 <sup>12</sup> |
| Instrument Cost (\$) <sup>c</sup>   | 10 <sup>7</sup>  | 10 <sup>6</sup>          | 10 <sup>7</sup>        | 10 <sup>6</sup>                  | 5 × 10 <sup>7</sup> ? | 10 <sup>5</sup>  |

<sup>a</sup> Inter-level alignment.

<sup>b</sup> Highly dependent on feature size for many techniques. Here we quote approximate numbers for features at the technique resolution.

<sup>c</sup> Approximate cost for basic state-of-the-art instrument, where available. This does not include the usage costs such as masks which can be significant and even dominant in a manufacturing mode.

**photolithography** is the method of choice for manufacturing in the microelectronics industry

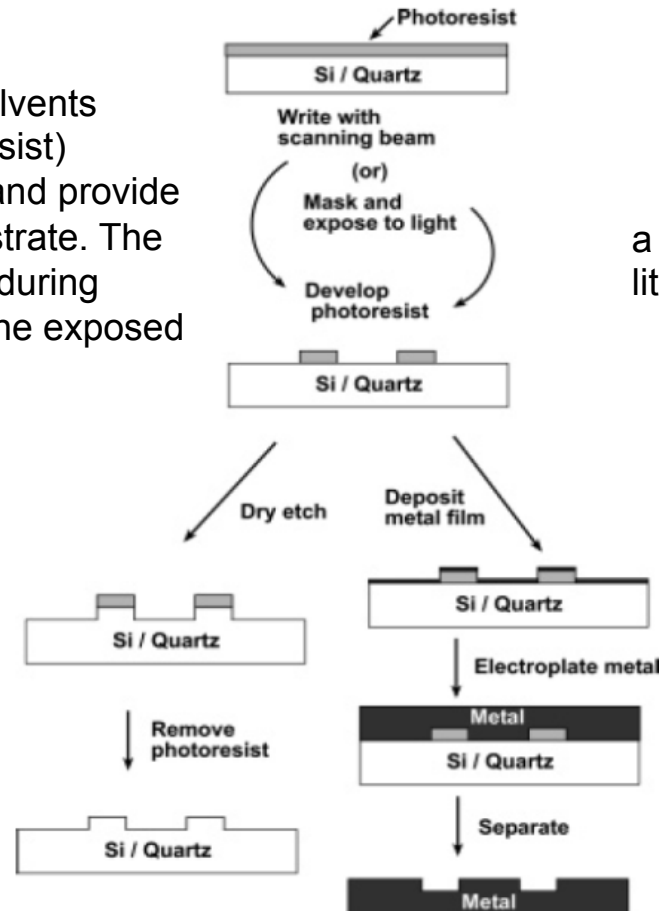


photoresit coated on a planar substrate, semiconductor wafer.

A **photoresist** is an organic material that cross links and becomes insoluble or that change chemically and becomes more soluble in a basic solution upon exposure to high-energy short-wavelength light (e.g. UV light)

max ~ 8 cm<sup>2</sup> in few seconds

The exposed photoresist is immersed in solvents that dissolve the exposed (positive photoresist) unexposed (negative photoresist) regions and provide patterned access to the surface of the substrate. The patterned photoresist masks the substrate during subsequent step that chemically modifies the exposed regions of the substrate.



a mask, typically patterned by scanning beam lithography, is used

**Figure 1.** Schematic illustration of the fabrication of topographically patterned surfaces in hard materials by conventional photolithography and electroplating.

to pattern smaller features, down to  $\sim 20$  nm, photolithography requires to decrease the imaging wavelength to 157 nm or to soft X-rays ( $\sim 13.5$  nm) known in the microelectronics industry as extreme ultraviolet (**EUV**) light. This change requires **new photoresists** to alter the wavelengths sensitivity and resolution of the resist as well as **new light sources** and, especially, **new types of optics** based on reflection rather than transmission to focus the light.

Scanning Beam Lithography is a slow process relative to photolithography.

- **scanned laser beams** with ~ 250-nm resolution are the least expensive
  - **focused electron beams** with sub-50-nm, expensive to purchase and maintain
  - **focused ion beam (FIB)** systems with sub-50-nm are primarily used in research
- This lithography technique can pattern features in a semiconductor with resolution down to ~20 nm and with the smallest lateral dimensions down to ~5 nm.

e-beam writing systems are very expensive >\$4M USD



## The new DANCHIP JEOL JBX-9300FS Electron Beam Lithography System



- Electron beam shape: Spot beam
- Accelerating voltage: 100 kV and 50 kV
- Schottkey gun emitter: ZrO/W (thermal field gun)
- Beam current: 50 pA – 100 nA
- Minimum beam size: 4 nm (100 kV), 7 nm (50 kV)
- Minimum feature size:  $\leq 20\text{nm}$  (100 kV),  $\leq 35\text{ nm}$  (50 kV)
- Overlay accuracy:  $\leq 30\text{nm}$
- Position accuracy:  $\leq 30\text{nm}$
- Wafer size: 50 – 300 mm
- Size of mask blank: 100 – 180 mm
- Writing method: Vector scan (random access)
- Writing field: Max. 500  $\mu\text{m}$  x 500  $\mu\text{m}$  (100 kV),
- Beam scanning speed: 40 ns to 4 ms/scanning increment

**mastering:** scanning-beam techniques are the principal methods of generating arbitrary nanoscale patterns

**replication:** photolithography is the principal method of transferring these patterns from one substrate to another

## limitations:

- these techniques come with high capital and operating costs
- limited accessibility to general users (incompatible with electronics fabrication)
- they are restricted to planar fabrication in semiconductor material
- incompatible with many problems in nonstandards fabrication
- the substrate is exposed to corrosive etchants, high energy radiation, relatively high temperatures
- non compatible with fragile materials such as organic and especially biological materials



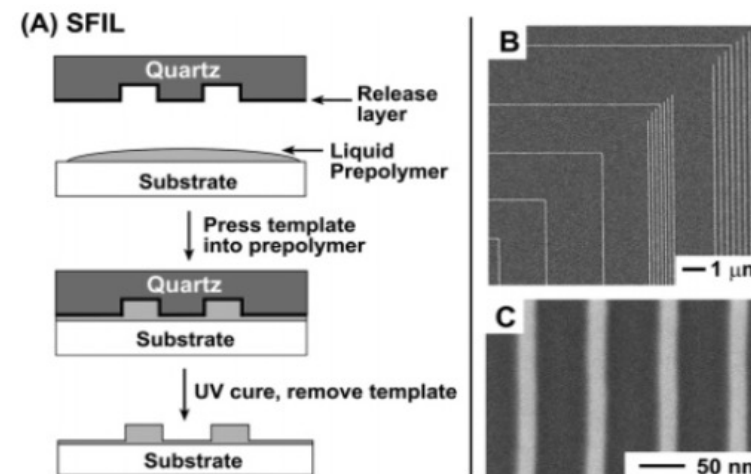
**development of unconventional techniques**

## Step-and-flash imprint lithography (SFIL)

Step-and-flash imprinted lithography is a technique that replicates the topography of a rigid mold using a photocurable prepolymer solution as the molded material

**hard mold:** made of silicon or quartz, thermally stable, chemically inert  
**release layer:** a fluorosilane  $[\text{CH}_3(\text{CF}_2)_6(\text{CH}_2)_2\text{SiCl}_3]$  is usually covalently linked to the surface of a hard mold to facilitate the release of the mold from the polymer and reduce surface fouling,

**quartz** is transparent to UV-light enabling photoinduced cross-linking of a molded prepolymer, silicon is not.

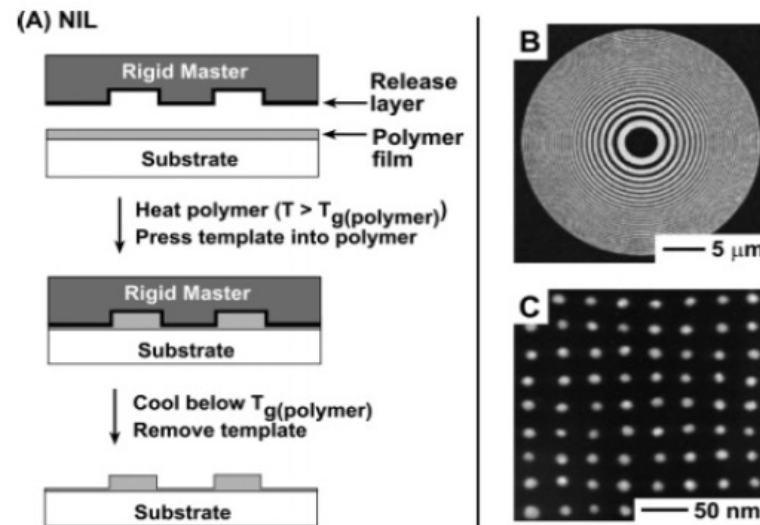


Schematic illustration of the procedure for step-and-flash imprint lithography (SFIL). Scanning electron microscopy (SEM) images of (B) 40-nm wide lines and (C) 20-nm wide lines patterned by step-and-flash lithography. The mold for the pattern in B was used for more than 1500 previous imprints.

for example, used for fabrication of metal oxide semiconductor field-effect transistor (MOSFET)

# Nanoimprinting Lithography (NIL)

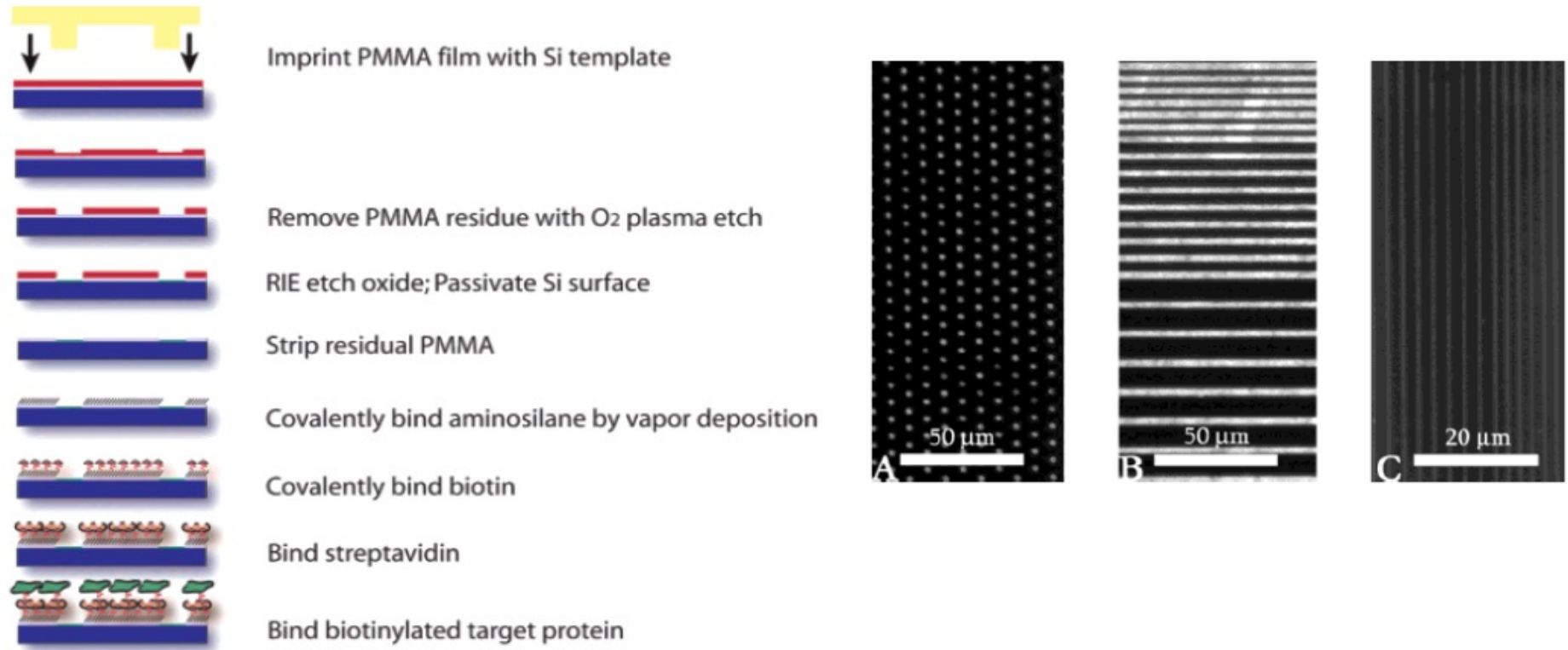
Nanoimprinting lithography refers to the pressure-induced transfer of a topographic pattern from a rigid mold (typically silicon) into a thermoplastic polymer film heated above its glass-transition temperature.



(A) Schematic illustration of nanoimprint lithography (NIL). The SEM images (B,C) show typical NIL experimental results. (B) Fresnel zone plates with a 125-nm minimum line width. (C) Metal dots with a 10-nm diameter and a periodicity of 40 nm.

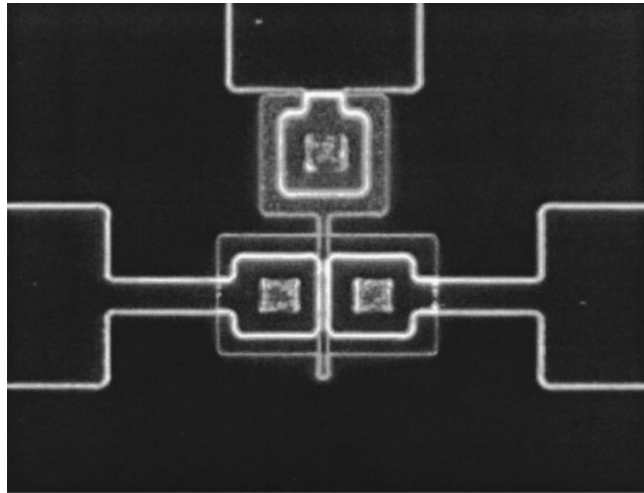
## Nanoscale Protein Patterning by Imprint Lithography

NANO LETTERS 2004, 4, 853-857



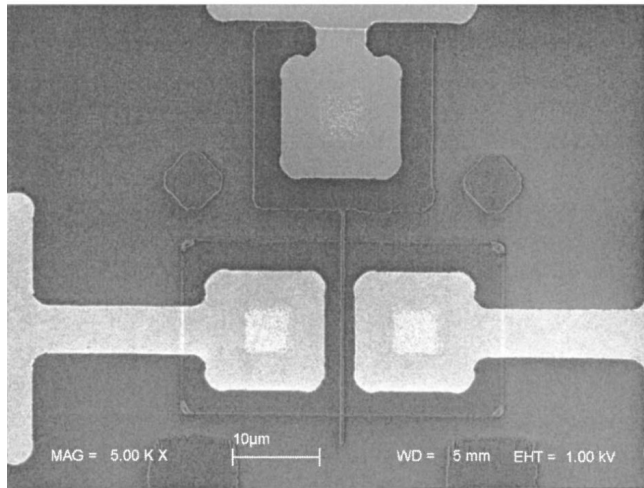
Process flow diagram of substrate patterning and protein immobilization. Spin-coated PMMA polymer is patterned by NIL. Exposed SiO<sub>2</sub> regions are etched and a passivating (CF<sub>x</sub>)<sub>n</sub> polymer ( $x = 1$  or  $2$ ,  $n =$  number of monomer subunits, monomer MW = 31 or 50) is deposited during a CHF<sub>3</sub> RIE (reactive ion etching) procedure. Residual PMMA is stripped away with acetone, exposing the underlying SiO<sub>2</sub> in the “patterned regions.” An aminosilane monolayer is covalently attached to the exposed “patterned regions”. Biotin-succinimidyl ester is then covalently linked to the primary amine of the aminosilane layer, and streptavidin is bound to the biotin layer. Finally, the biotinylated target protein is bound to the streptavidin layer.

## Fabrication of 60-nm transistors



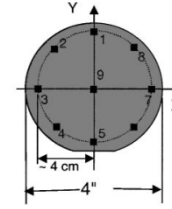
(a)

5 μm



(b)

The images of the MOSFETs fabricated by using NIL at all (four) lithographic levels. (a) Dark-field optical image of a 1- $\mu\text{m}$ -gate-length MOSFET. (b) The SEM image of a 60-nm-channel-length MOSFET. (Note: The overlay accuracy among the layers is within 0.5 mm in both X and Y directions in the images.)

Data in X-Direction: ( $\mu\text{m}$ )

| Run #                                     | 1          | 2          | 3          | 4          | 5          | 6          | 7          | 8          | 9          | Ave <sub>s</sub> | $\sigma_s$ |
|---|------------|------------|------------|------------|------------|------------|------------|------------|------------|------------------|------------|
| 1   | -1         | -0.5       | 0          | +0.25      | +0.5       | 0          | -0.5       | -1         | -0.5       | 0.5              | 0.3        |
| 2   | +1         | +1         | +0.5       | 0          | -0.5       | -0.5       | 0          | +1         | +0.5       | 0.5              | 0.4        |
| 3   | +1.5       | +1.5       | +1         | 0          | -0.5       | 0          | +0.5       | +1         | +0.5       | 0.8              | 0.6        |
| 4   | -1         | -1         | -0.5       | -0.5       | 0          | -0.5       | -0.5       | -0.5       | -0.5       | 0.5              | 0.3        |
| 5   | -0.5       | -0.5       | -0.5       | -0.5       | -0.5       | -0.5       | 0          | 0          | 0          | 0.3              | 0.2        |
| 6   | +0.25      | 0          | +0.5       | +1         | +0.75      | +0.5       | +0.5       | 0          | +0.5       | 0.4              | 0.3        |
| 7   | -1         | -1         | -0.5       | 0          | +0.25      | 0          | -0.5       | -1         | -0.25      | 0.5              | 0.4        |
| 8   | +0.5       | 0          | -0.5       | -0.5       | +0.5       | -0.5       | -0.5       | +0.25      | -0.25      | 0.3              | 0.2        |
| <b>Ave<sub>multi</sub></b>                | <b>0.7</b> | <b>0.7</b> | <b>0.6</b> | <b>0.4</b> | <b>0.6</b> | <b>0.4</b> | <b>0.4</b> | <b>0.6</b> | <b>0.5</b> | <b>0.5</b>       |            |
| <b><math>\sigma_{\text{multi}}</math></b> | <b>0.3</b> | <b>0.5</b> | <b>0.4</b> | <b>0.4</b> | <b>0.2</b> | <b>0.3</b> | <b>0.4</b> | <b>0.4</b> | <b>0.3</b> | <b>0.2</b>       |            |

Data in Y-Direction: ( $\mu\text{m}$ )

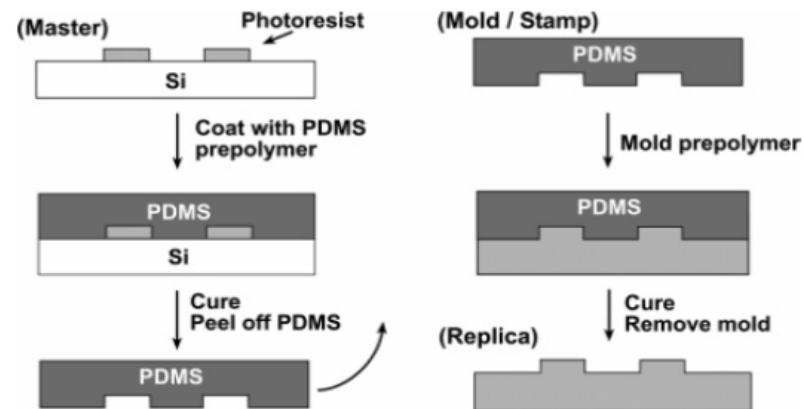
| Run #                                     | 1          | 2          | 3          | 4          | 5          | 6          | 7          | 8          | 9          | Ave <sub>s</sub> | $\sigma_s$ |
|---|------------|------------|------------|------------|------------|------------|------------|------------|------------|------------------|------------|
| 1   | +1.5       | +1         | +1.25      | +1.25      | +1.5       | +1.5       | +2         | +1.5       | +1.5       | 1.3              | 0.4        |
| 2   | -0.5       | -0.5       | 0          | 0          | -0.5       | -0.5       | -1         | +1         | -0.5       | 0.6              | 0.3        |
| 3   | +1         | +1         | +1.5       | +1.5       | +1         | 0          | 0          | 0          | +0.5       | 0.7              | 0.6        |
| 4   | +1         | +1         | +1         | +1.5       | +1.5       | +1.5       | +1.5       | +1         | +1         | 1.2              | 0.2        |
| 5   | 0          | 0          | 0          | 0          | 0          | -0.5       | 0          | 0          | 0          | 0.1              | 0.2        |
| 6   | 0          | 0          | 0          | 0          | 0          | 0          | 0          | 0          | 0          | 0                | 0          |
| 7   | +0.5       | 0          | 0          | 0          | 0          | +0.5       | +1         | +1         | +0.25      | 0.4              | 0.3        |
| 8   | 0          | 0          | 0          | 0          | 0          | -0.5       | -0.5       | -0.5       | 0          | 0.2              | 0.2        |
| <b>Ave<sub>multi</sub></b>                | <b>0.7</b> | <b>0.6</b> | <b>0.6</b> | <b>0.6</b> | <b>0.6</b> | <b>0.8</b> | <b>0.9</b> | <b>0.8</b> | <b>0.6</b> | <b>0.6</b>       |            |
| <b><math>\sigma_{\text{multi}}</math></b> | <b>0.5</b> | <b>0.5</b> | <b>0.6</b> | <b>0.6</b> | <b>0.6</b> | <b>0.6</b> | <b>0.7</b> | <b>0.6</b> | <b>0.5</b> | <b>0.5</b>       |            |

The overlay accuracies and the statistics of all (eight) consecutive lithography runs for multilayer NIL in the nano-MOSFETs fabrications. The data came from two finished wafers and one unfinished wafer. The numbers in the first row of the table are corresponding to the nine locations over the 4-in. wafer shown in the top schematic. The overall statistical average is 0.5  $\mu\text{m}$  with a standard deviation of 0.2  $\mu\text{m}$  in the X-direction, and 0.6  $\mu\text{m}$  with a standard deviation of 0.5 mm in the Y-direction.

Techniques that prepare a soft mold or stamp by casting a liquid polymer precursor against a topographically patterned master are commonly referred to as **soft lithography**.

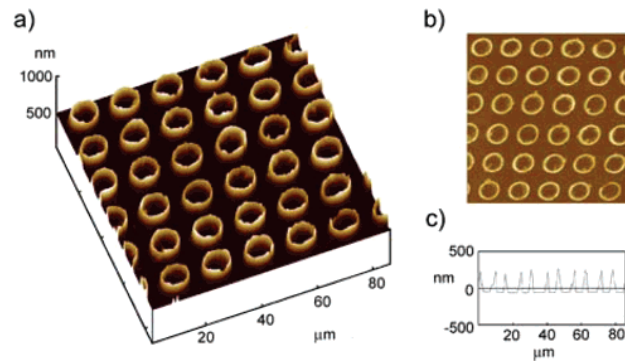
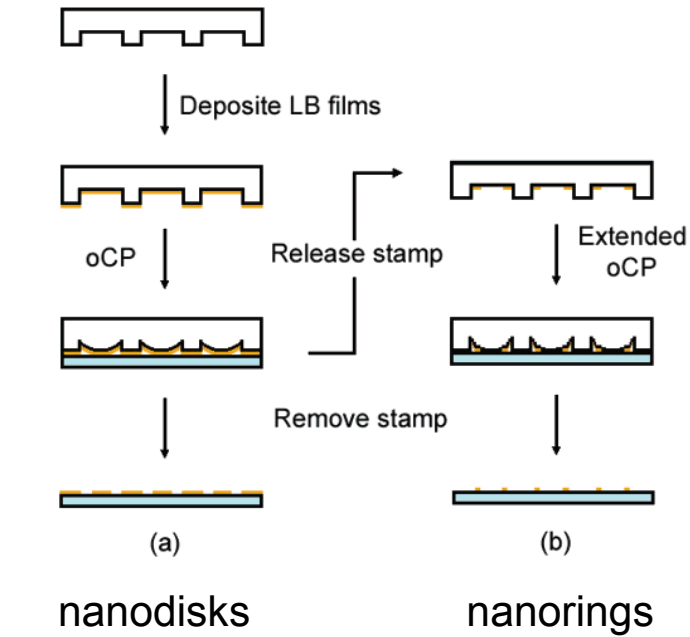
**PDMS** = poly(dimethylsiloxane). This material is durable, unreactive toward most materials being patterned or molded, chemically resistant to many solvents and transparent above 280 nm. One of the major advantages of PDMS is that fabrication of molds or stamps (by replica molding) is so **inexpensive** that a large number of uses may not be necessary. Infact, sometimes the mold or stamp becomes a **disposable reagent**.

An important limitation of PDMS is that it absorbs many nonpolar, low-molecular-weight organic compounds.

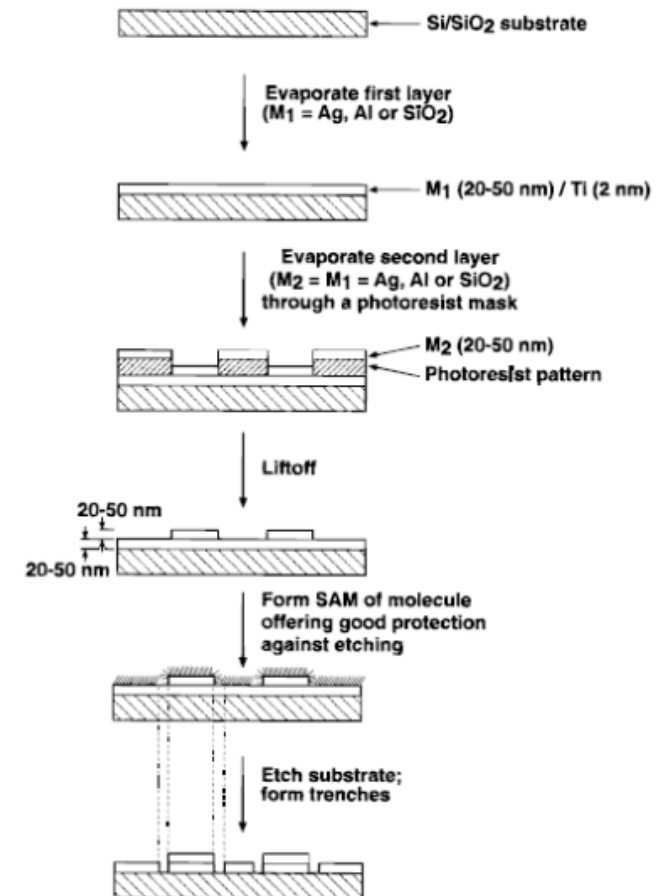


Schematic illustration of the formation of topographically patterned molds (or stamps, depending on the application) and replication of the master into a third functional material.

## Overpressure microcontact printing



## Defect patterning





Different techniques may be used:

## Replica Molding

## Solvent-assisted Micromolding (SAMIM)

This process has been demonstrated for a number of polymers including Novolac photoresists, PS, PMMA, cellulose acetate poly(vinyl chloride) (PVC).

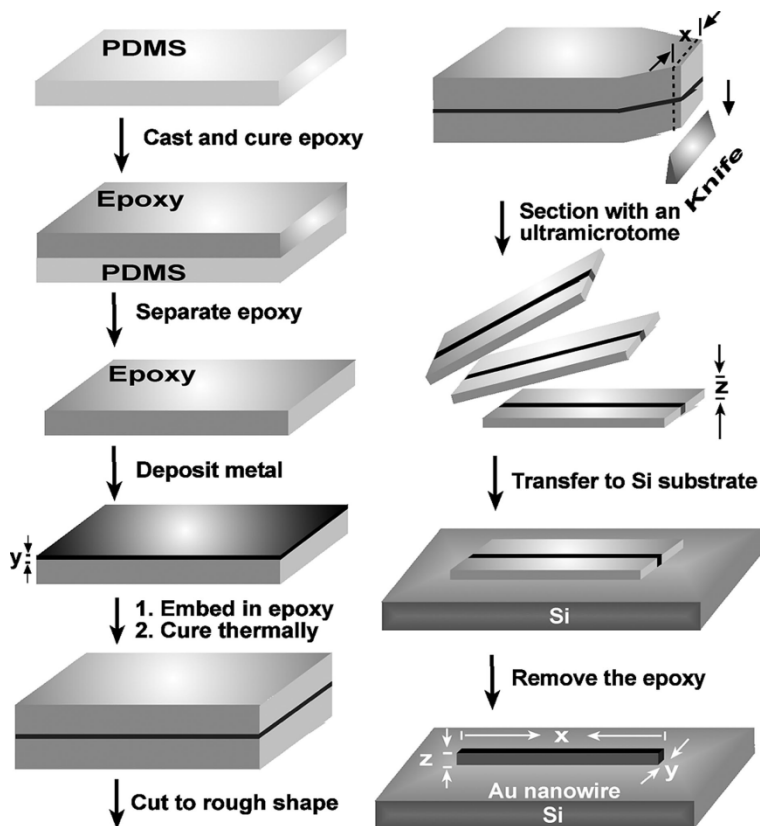
The mild processing conditions of SAMIM are compatible with patterning polymer-based distributed feedback lasers and organic light-emitting diodes (OLEDs).

## limits:

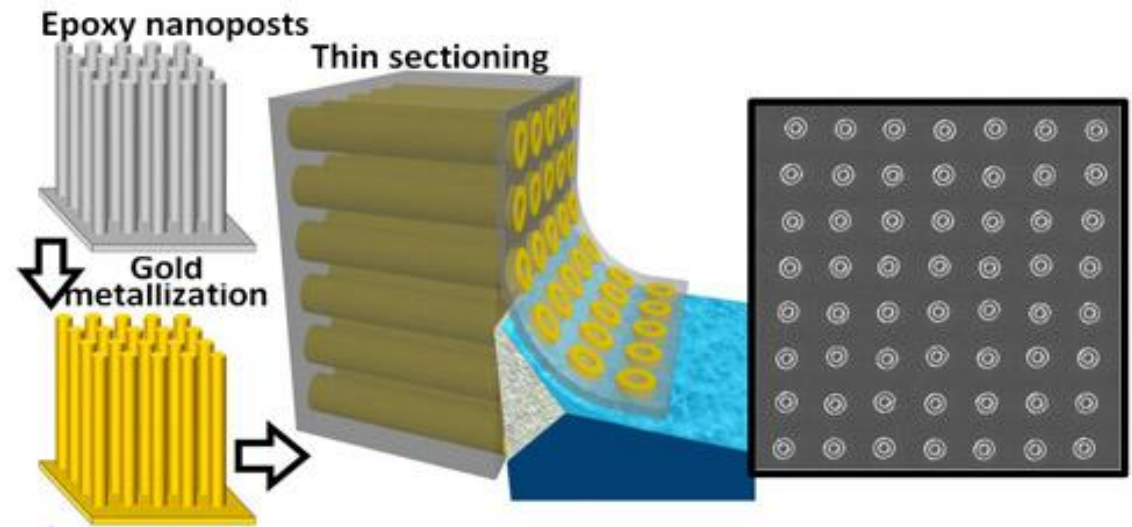
- the practicality of fabricating masters with small features
- the ability of a material to mold, with high fidelity, the features of the master
- the distortion of features in the transferred pattern
- the swelling of the master by the monomers used or the solvent used to dissolve polymers
- the ability of the molded material to fill the mold completely

Molding and embossing are the most widely pursued and successful techniques for unconventional nanofabrication

## Nanoskiving

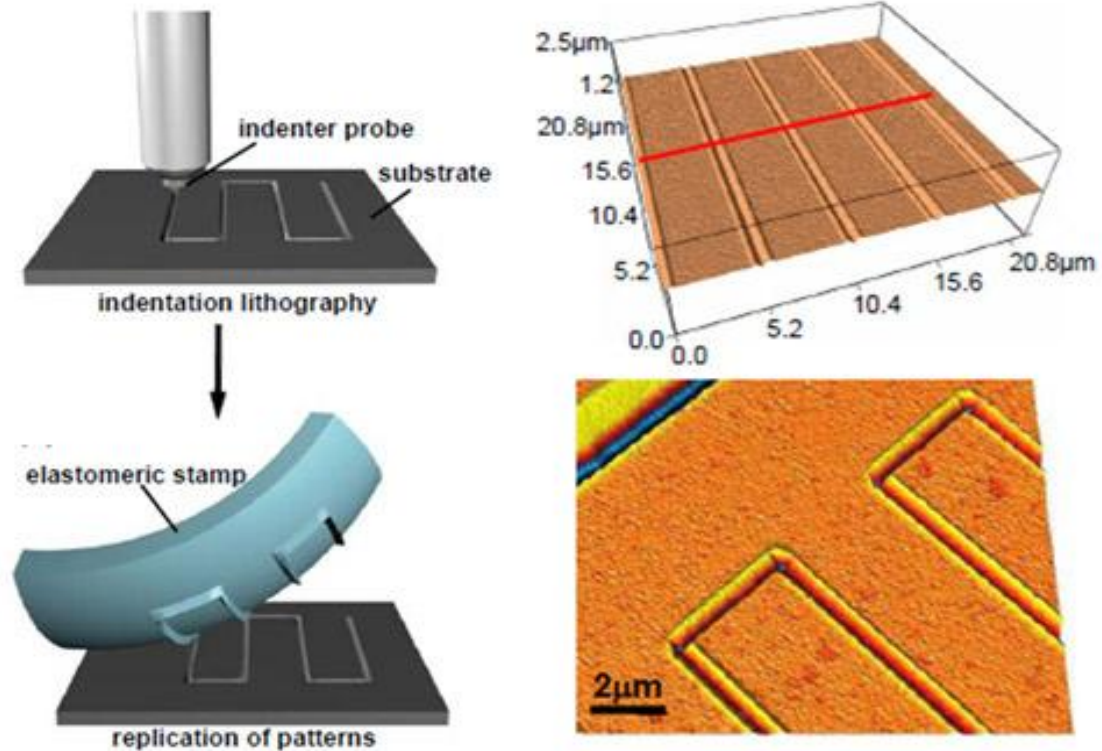


## soft pattern transfer elements

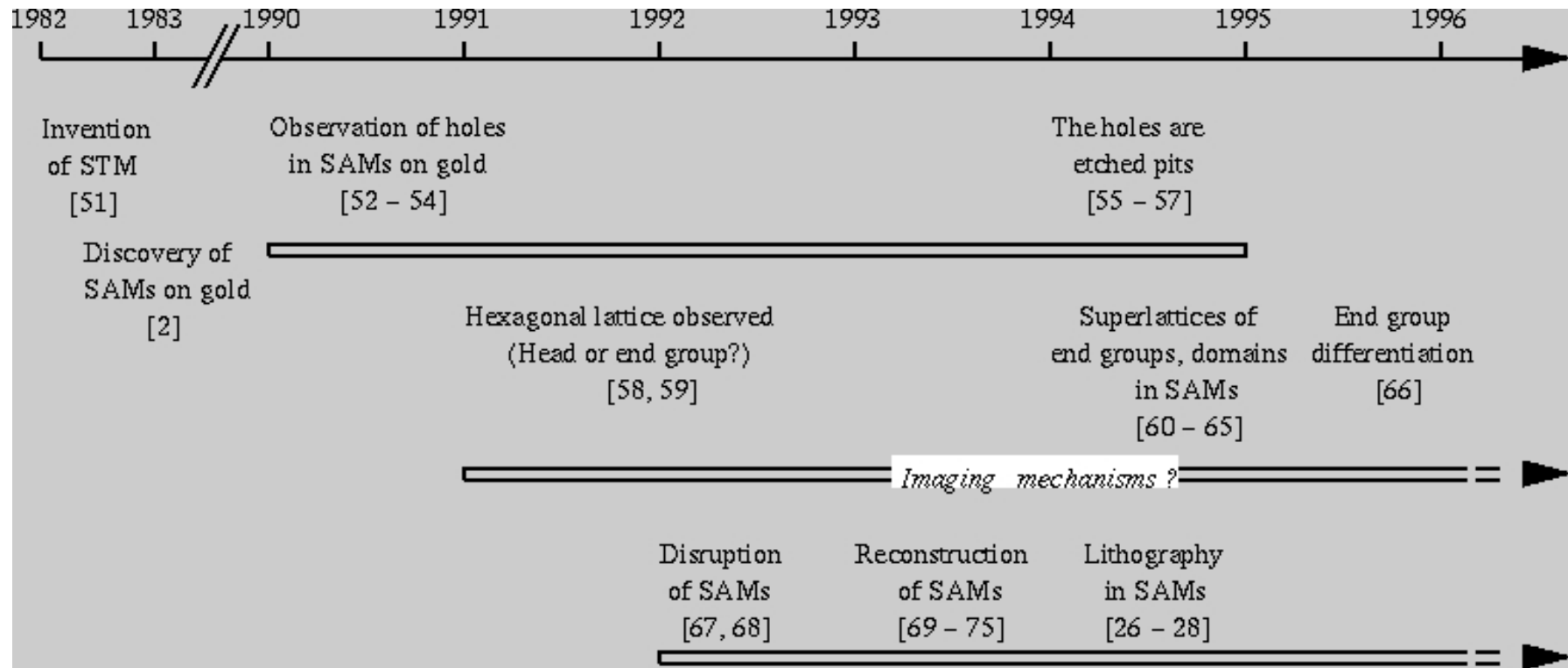


Fabrication of gold nanorings arrays by nanoskiving.

Fabrication of metal nanowires by nanoskiving. This procedure begins with the replication of a flat or topographically patterned PDMS surface in epoxy, followed by the deposition of a thin film of metal on the epoxy by e-beam evaporation or sputtering. The topography of the original template determines the dimension along the  $x$ -direction. The thickness of the evaporated metal film determines the dimension in the  $y$ -direction and can be as small as 20 nm for gold. After embedding the thin metallic film in more epoxy and curing, sectioning with an ultramicrotome produces sections with a thickness ( $z$ ) as small as 50 nm using a standard  $45^\circ$  diamond knife. After sectioning, transfer of the epoxy section to a silicon substrate and removal of the epoxy with an oxygen plasma leaves free-standing metal nanostructures. The  $y$  and  $z$ -dimensions of these nanostructures throughout the paper are as defined in the figure.



Nanoindentation process to fabricate nanochannels and use them as master for elastomeric stamps.

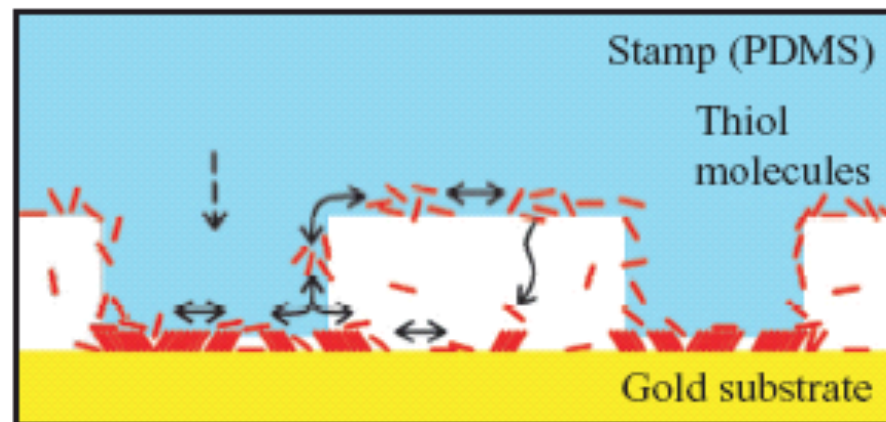
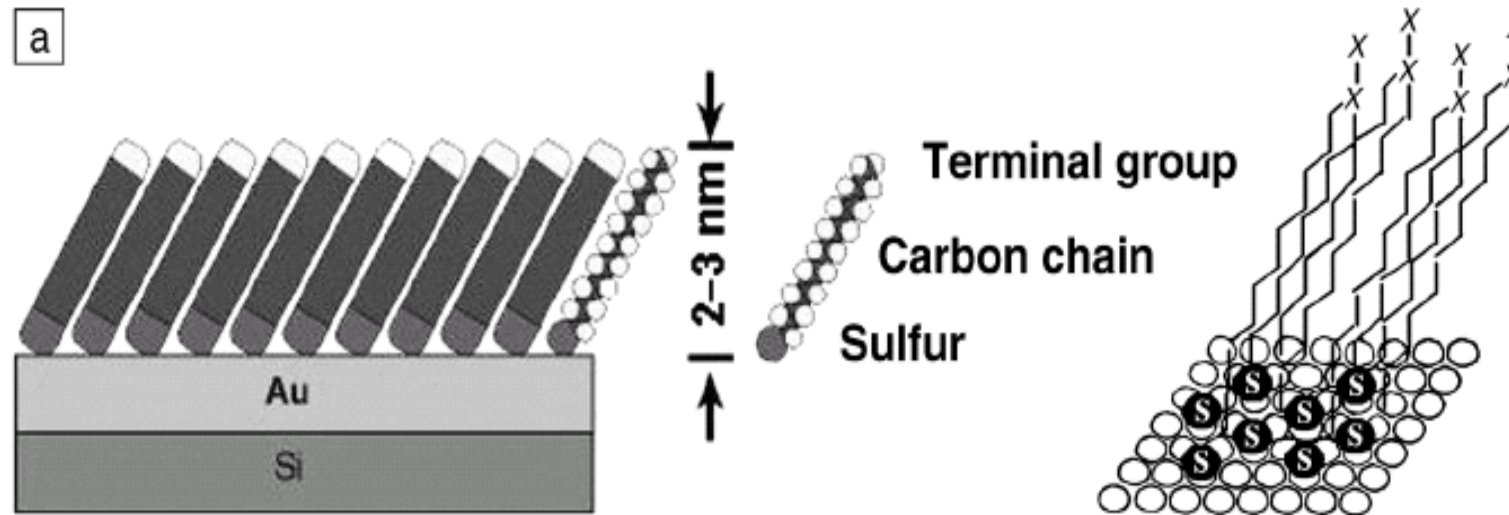


## **Microfabrication by microcontact printing of self-assembled monolayers**

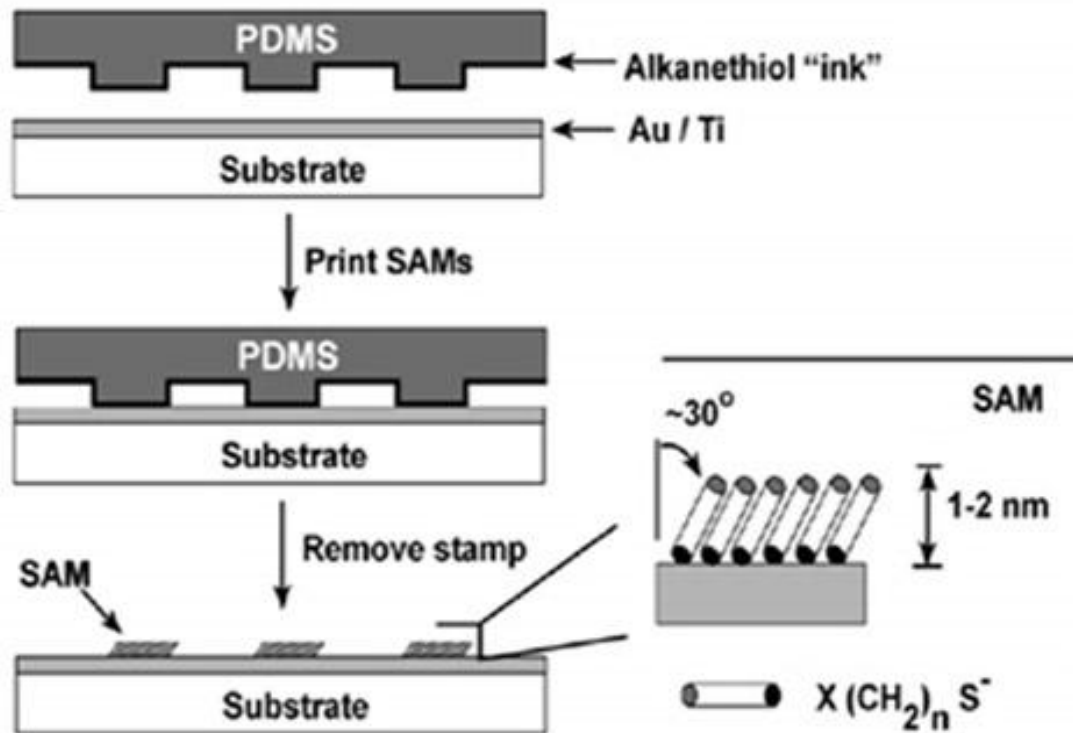
G.M. Whitesides et al. Adv. Mater. 1994, 6, 600.

Microcontact printing offers extreme experimental simplicity and flexibility, relying on the ability of self-assembled monolayers of long chain alkanethiolates on gold and others metals to act as nanometer resists.

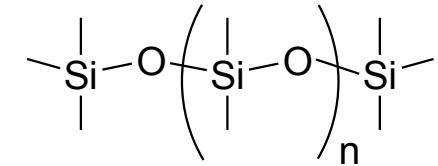
## Self-Assembled Monolayers (SAMs): an Ink



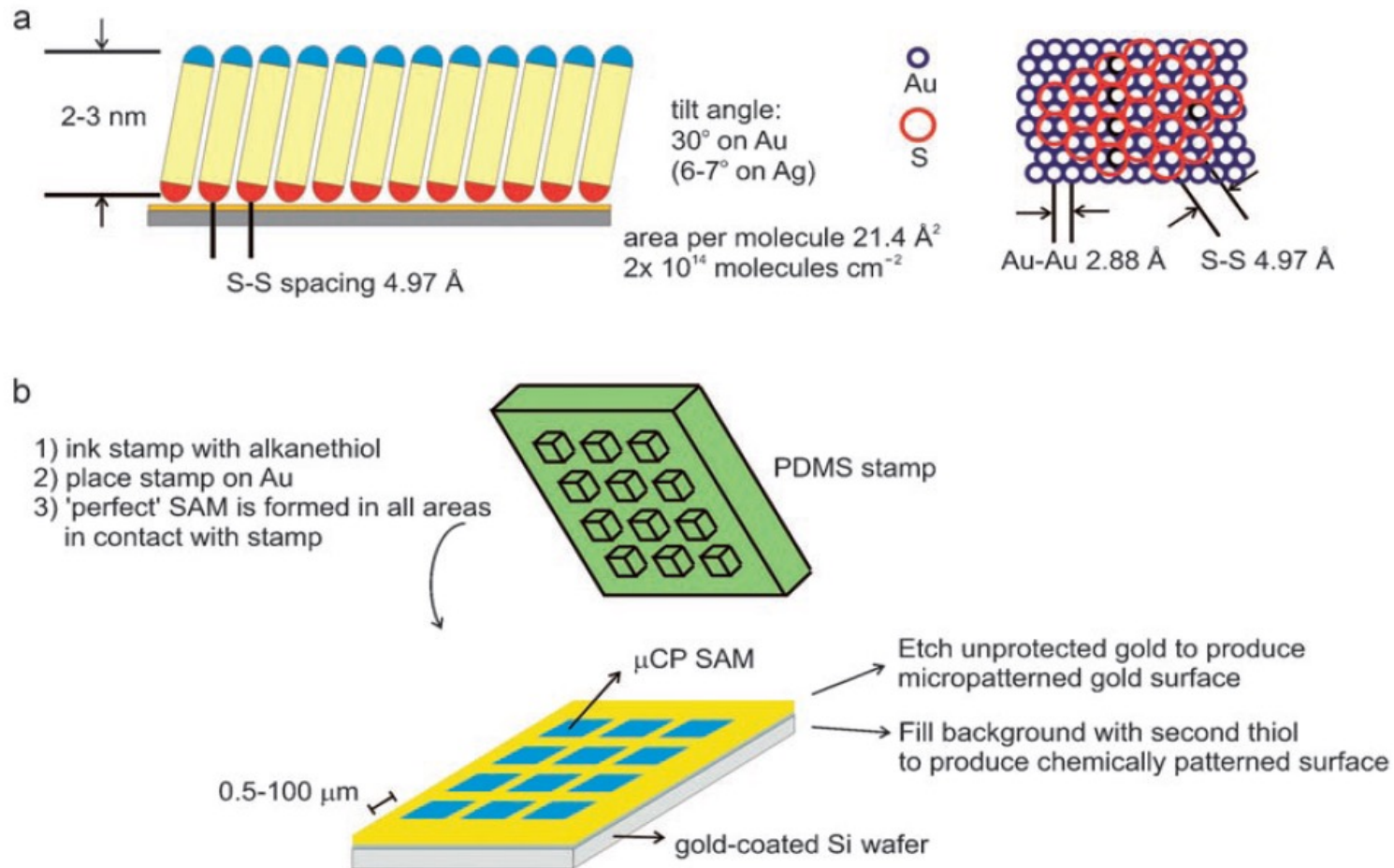
Xia, Y.; Whitesides, G. M. *Angew. Chem., Int. Ed.* **1998**, *37*, 550.  
Michel, B.; Bernard, A., et al. *IBM J. Res. & Dev.* **2001**, *45*, 697.

Microcontact Printing ( $\mu$ CP)

PDMS = poly(dimethylsiloxane)



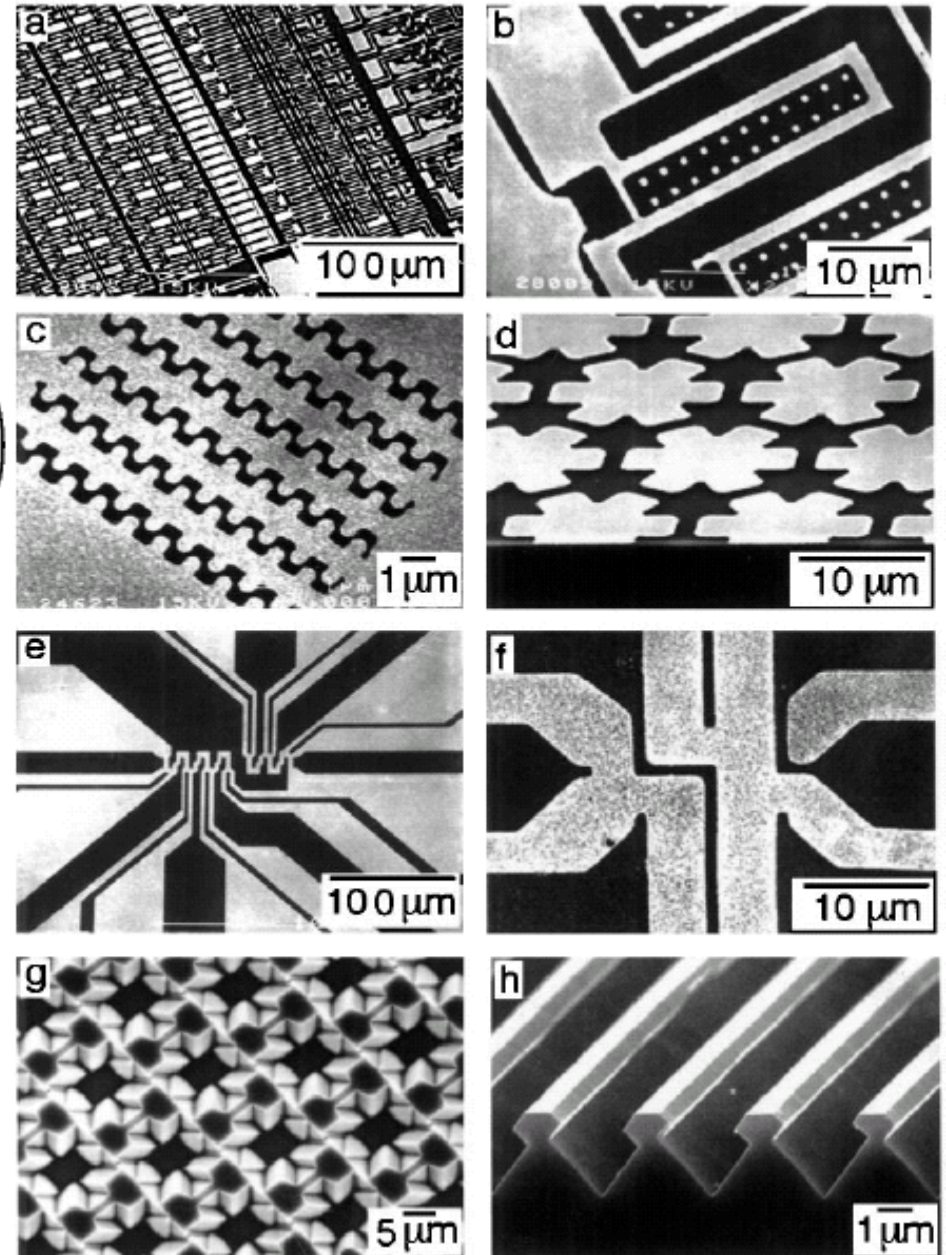
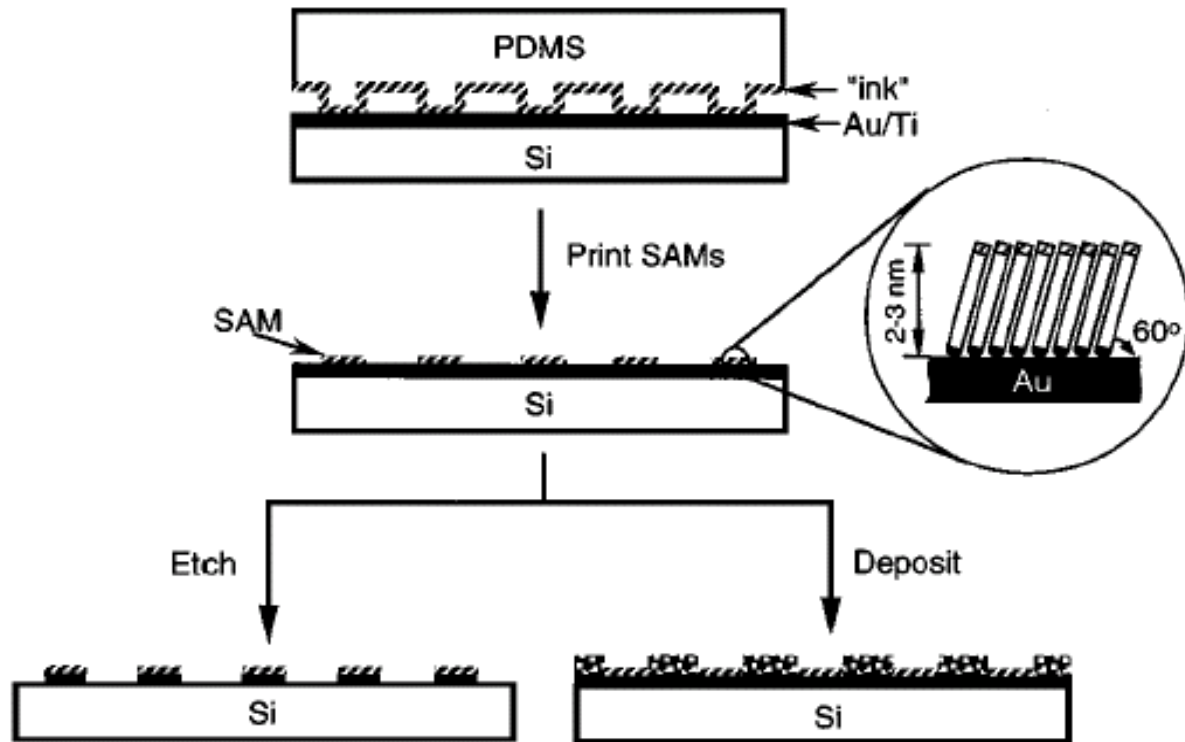
Nanofabrication by stamping. Microcontact printing ( $\mu$ CP) transfers molecules from a patterned PDMS stamp to a substrate by the formation of covalent bonds. Electrical microcontact printing (e- $\mu$ CP) uses a flexible electrode to pattern a thin film of a material that is an electret (i.e., that accepts and maintains an electrostatic potential), probably by injecting and trapping charges.

Microcontact Printing ( $\mu$ CP)

**Figure 1.** a) Structure of self-assembled monolayers (SAMs) of alkanethiolates on gold, and b) formation of patterned SAMs using microcontact printing ( $\mu$ CP). PDMS = poly(dimethyl siloxane).



## Microcontact Printing ( $\mu$ CP)



Xia, Y.; Whitesides, G. M. *Ann. Rev. Mater. Sci* **1998**, 28, 153.

a-c: Silver; e: Gold; f: copper; a+b: rolling stamp;  
g+h: metal as etch mask for silicon.

## High-Speed Microcontact Printing

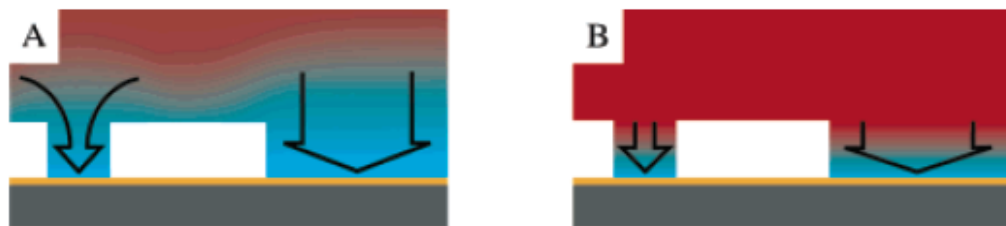


**Figure 1.** Schematic comparison of ink concentrations in stamps after printing. (A) Low ink concentrations and long printing times result in a depletion layer (blue) that extends beyond the protrusions. (B) Fast printing using high ink concentrations leads to a narrow depletion layer. As a result, the ink flux is independent of the stamp pattern.

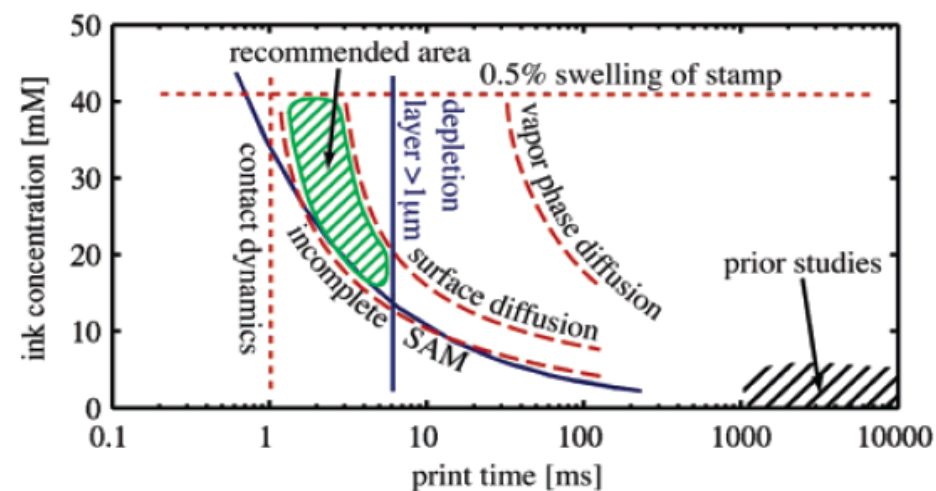
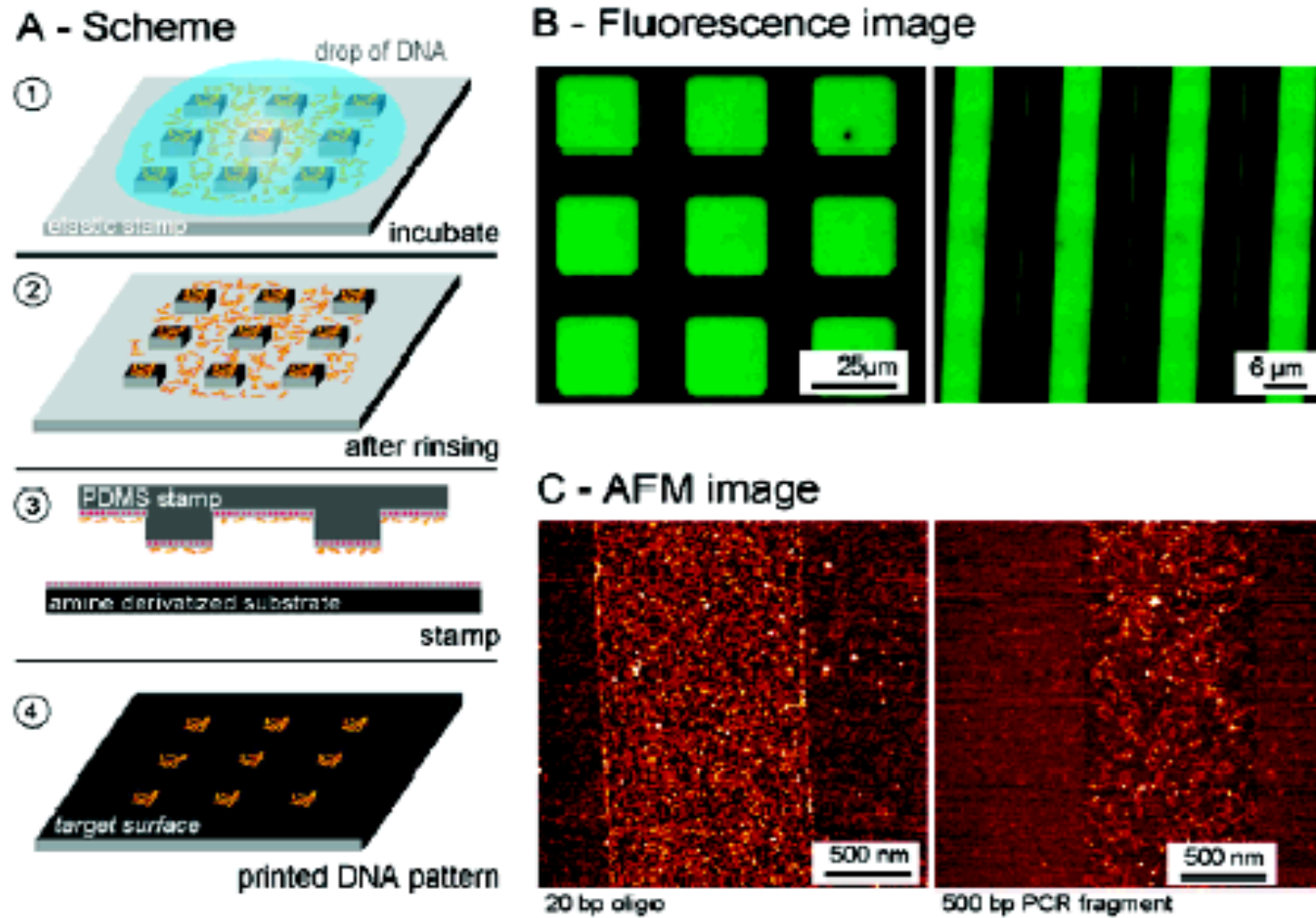


**Figure 4.** Semiquantitative graph illustrating the process window of high-speed  $\mu$ CP. The recommended parameter space is confined by the limits of contact dynamics, the distortion of the stamp due to ink-induced swelling (red dotted lines), the condition for complete SAM formation (blue solid line, simulation; red dashed line, experiment), and surface diffusion, whereas vapor-phase diffusion is not a limiting factor (red dashed lines). Fill-factor-independent ink flux is possible on the left side of the vertical blue line (simulation for 1  $\mu$ m thick depletion layer<sup>6</sup>).

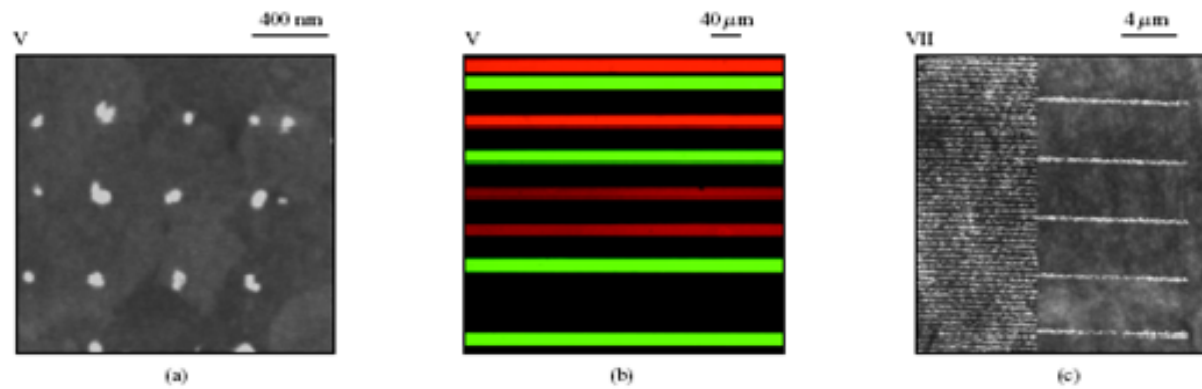
J. A. Helmuth, H. Schmid, R. Stutz, A. Stemmer,  
H. Wolf, *J. Am. Chem. Soc.* **2006**, *128*, 9296-9297.

## Microcontact Printing DNA



S.A. Lange, V. Benes, D.P. Kern, J.K.H. Horber, A. Bernard, *Anal. Chem.* **2004**, 76, 1641.

## Microcontact Printing with Proteins



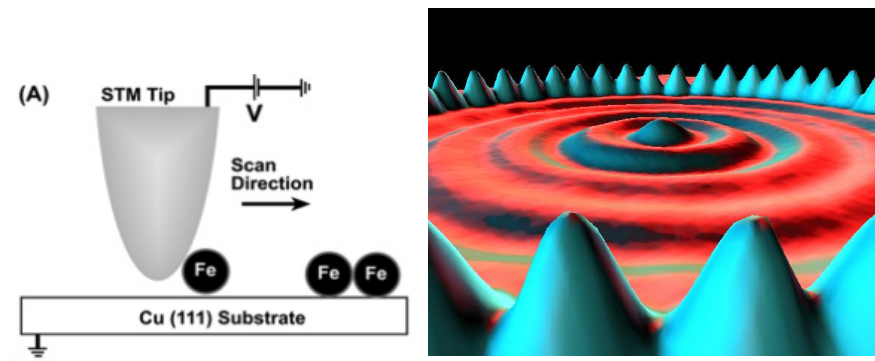
H. Wolf et al. *IBM Journal of Research & Development*. 2001, 45, 697.

# Scanning Probe Litography (SPL)

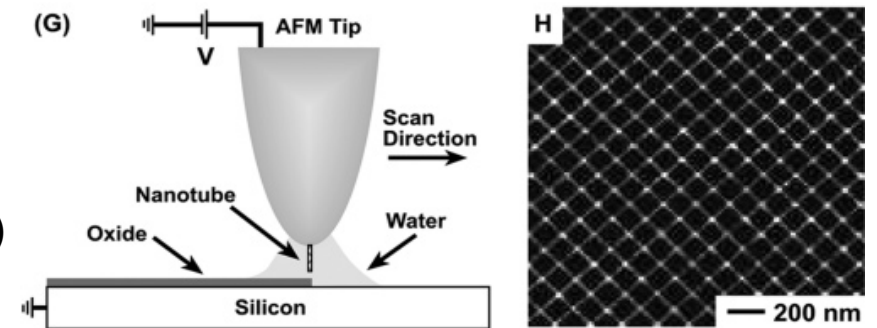
Scanning Probe Litography provides a versatile set of tools for both manipulating and imaging the topography of a surface with atomic-scale resolution.

the most important techniques include:

- scanning tunneling microscopy (**STM**)
- atomic force microscopy (**AFM**)
- near-field scanning optical microscopy (**NSOM**)

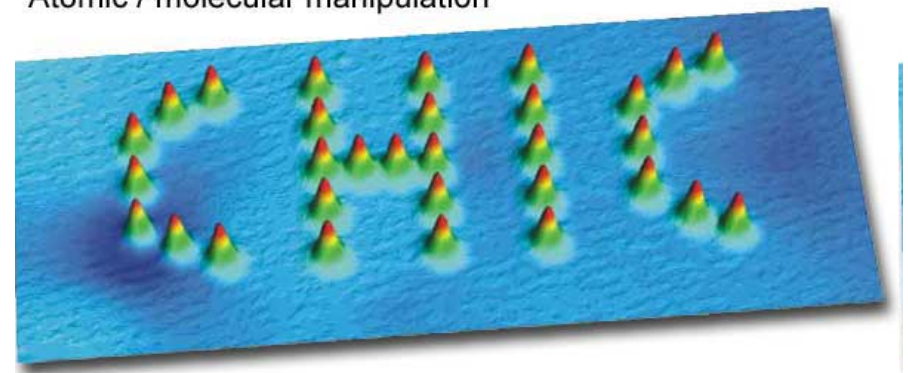


Scanning tunneling microscopy (STM) can position atoms on a surface with high precision to generate patterns, such as (B) a quantum corral of a 48-atom Fe ring formed on Cu enclosing a defect-free region.

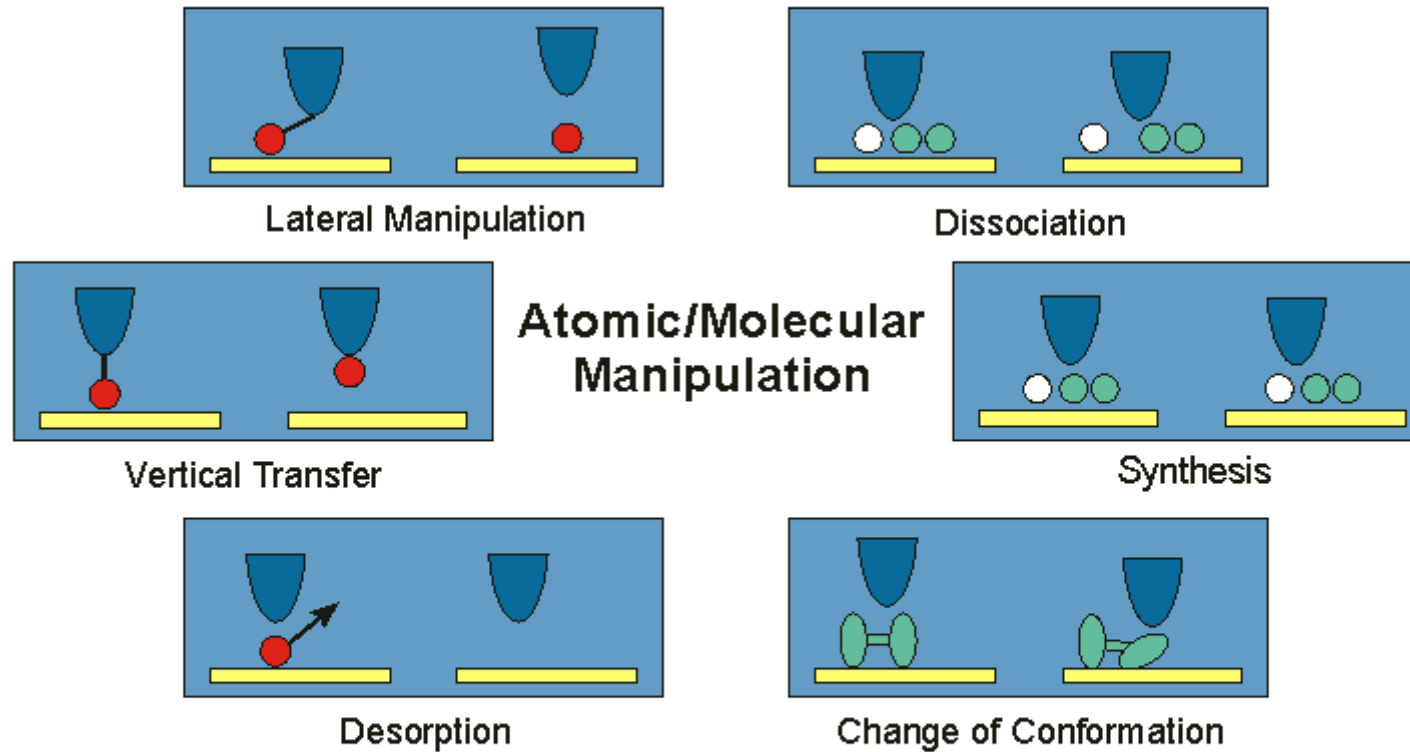


Scanning electrochemical oxidation with a carbon nanotube-modified AFM tip can selectively oxidize a surface to pattern (H) 10-nm wide (2-nm tall) silicon oxide lines spaced by 100 nm.

Atomic / molecular manipulation

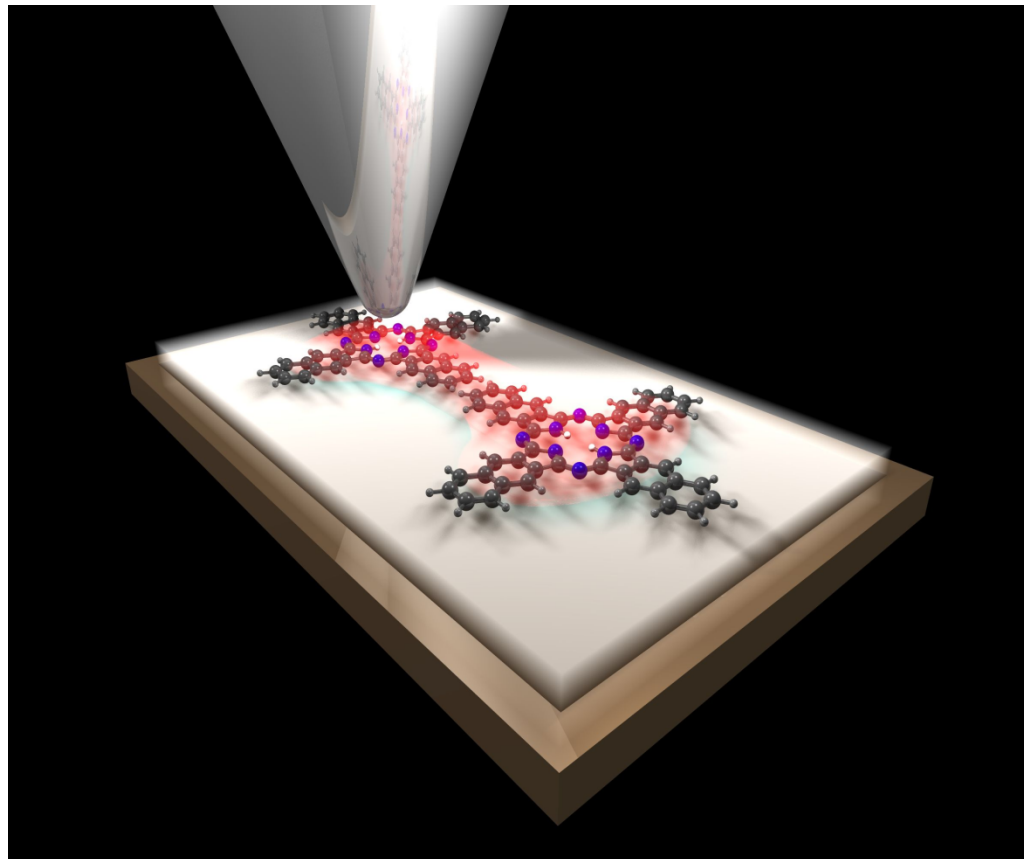


Example 1: Individual Cu atoms on Cu(111).  
Size: 25 x 8 nm<sup>2</sup>.



Overview of manipulation processes.

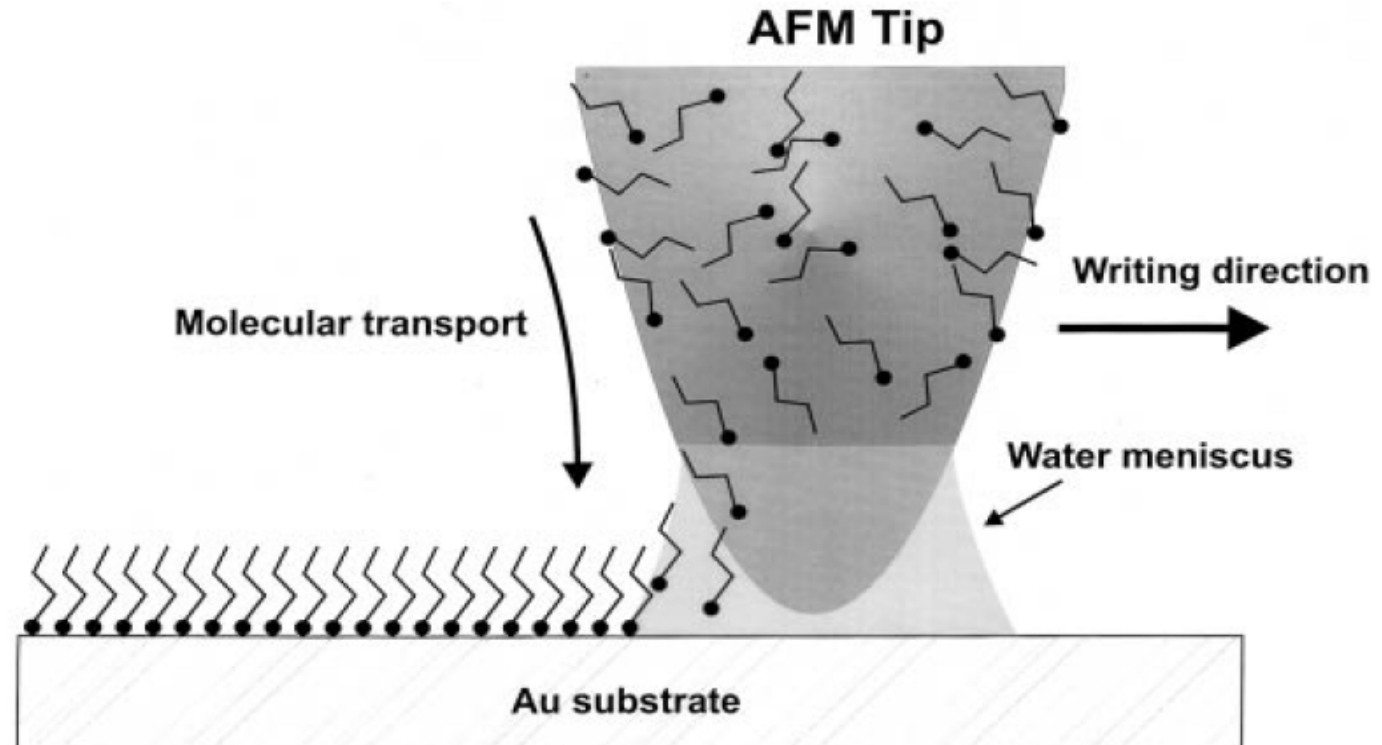
Schematic view of two coupled naphthalocyanine molecules probed by the tip of a low-temperature scanning tunneling microscope.



By increasing the bias voltage between the tip and the sample, a hydrogen tautomerization reaction could be induced by the tunnelling electrons in the STM junction. Although the molecule itself does not rotate, this change is formally equivalent to the rotation of the molecule by  $90^\circ$  and causes a significant change in the tunnelling current measured at the STM tip positioned over the molecule. We have also demonstrated that switching can be even induced by injecting electrons into adjacent molecules. As the switching is well-defined, highly localized, reversible, intrinsic to the molecule, and does not involve changes in the molecular frame, this class of molecules can be used as building blocks for more complex molecular devices such as logic gates.

## DIP-PEN NANOLITHOGRAPHY (DPN)

**Fig. 1.** Schematic representation of DPN. A water meniscus forms between the AFM tip coated with ODT and the Au substrate. The size of the meniscus, which is controlled by relative humidity, affects the ODT transport rate, the effective tip-substrate contact area, and DPN resolution.

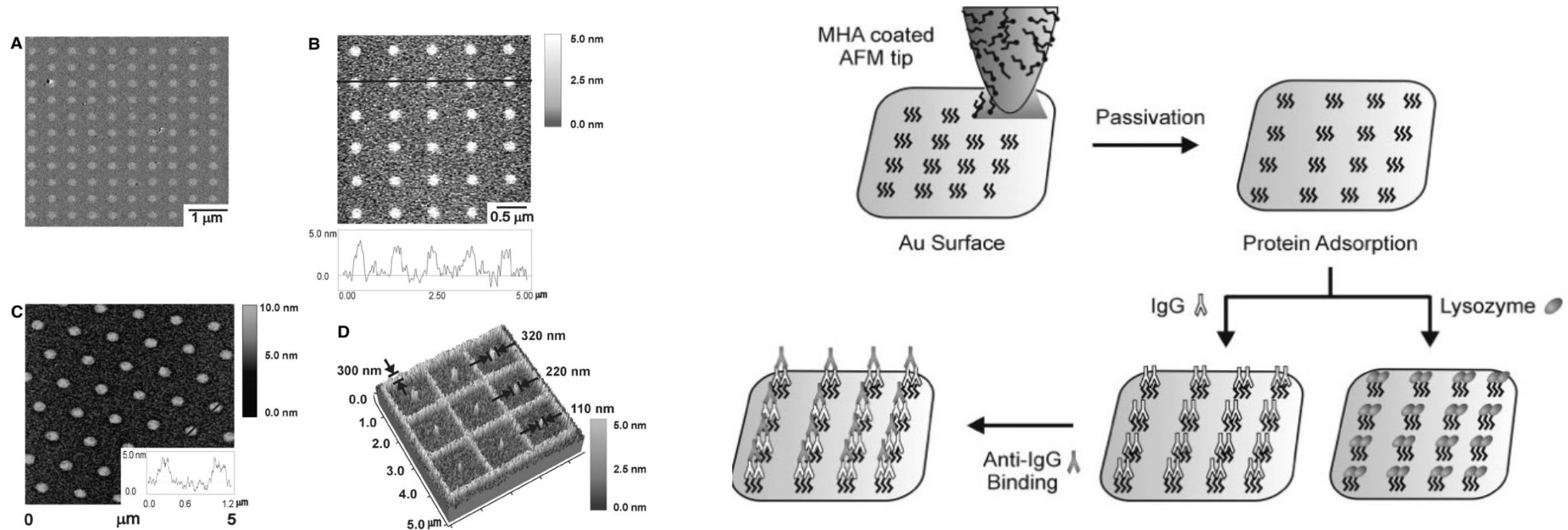


R. D. Piner, J. Zhu, F. Xu, S. Hong, C. A. Mirkin SCIENCE VOL 283 29 JANUARY 1999, 661



## DIP-PEN NANOLITHOGRAPHY (DPN)

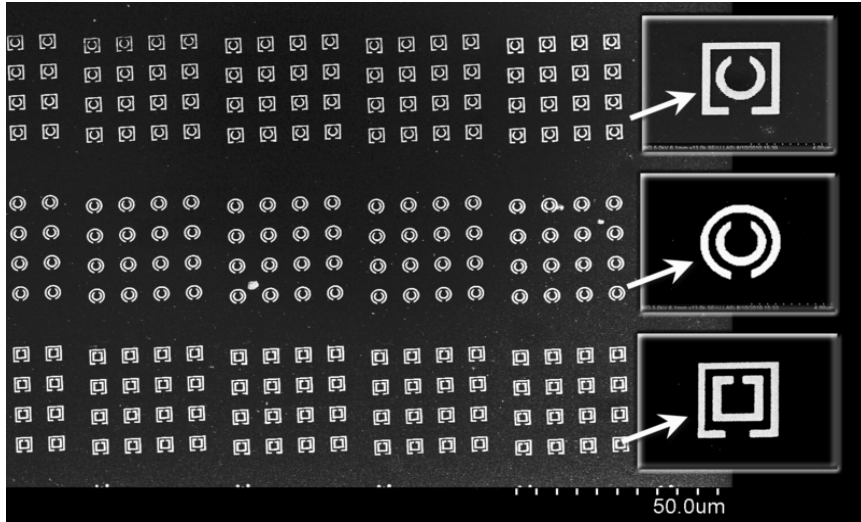
### Protein Nanoarrays Generated by Dip-Pen Nanolithography



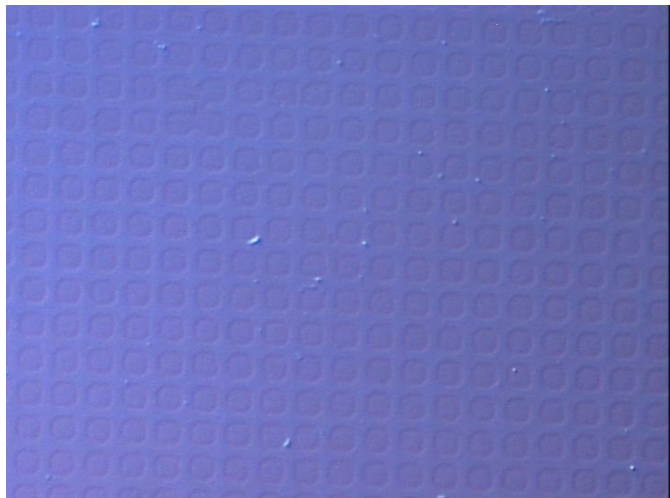
AFM images and height profiles of lysozyme nanoarrays. **(A)** Lateral force image of an 8 μm by 8 μm square lattice of MHA dots deposited onto an Au substrate. The array was imaged with an uncoated tip at 42% relative humidity (scan rate = 4 Hz). **(B)** Topography image (contact mode) and height profile of the nanoarray after lysozyme adsorption. A tip-substrate contact force of 0.2 nN was used to avoid damaging the protein patterns with the tip. **(C)** A tapping mode image (silicon cantilever, spring constant = ~40 N/m) and height profile of a hexagonal lysozyme nanoarray. The image was taken at a scan rate of 0.5 Hz to obtain high resolution. **(D)** Three-dimensional topographic image of a lysozyme nanoarray, consisting of a line grid and dots with intentionally varied feature dimensions. Imaging was done in contact mode as described in (B).

Diagram of proof-of-concept experiments, in which proteins were absorbed on preformed MHA patterns. The resulting protein arrays were then characterized by AFM.

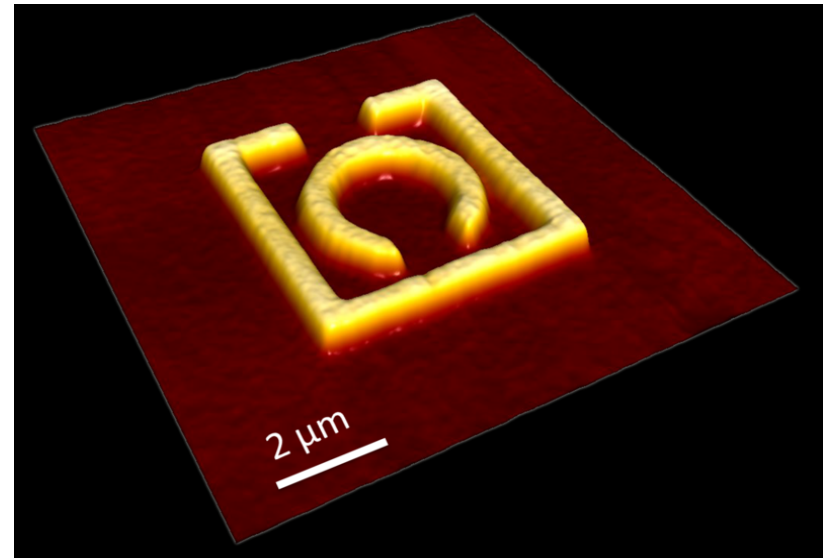
K.-B. Lee, S.-J. Park, C. A. Mirkin, J. C. Smith, M. Mrksich *Science* **2002**, 295, 1702.



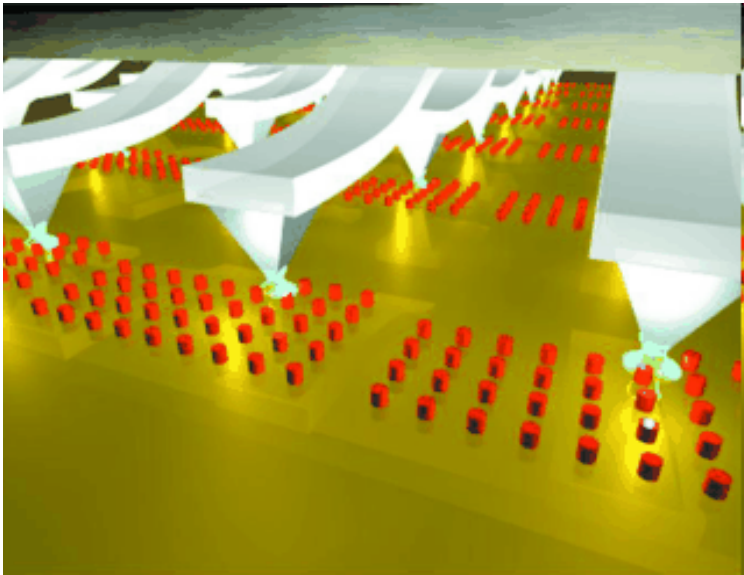
SEM image of DPN fabricated gold metastructure arrays.



Streptavidin (4nm thickness) deposited using micro contact printing



Gold on silicon metastructure fabricated with top-down DPN methods



55 000-pen 2D array

## Massively Parallel Dip-Pen Nanolithography with 55000-Pen Two-Dimensional Arrays

K. Salaita, Y. Wang, J. Fragala, R. A. Vega, C. Liu, and C. A. Mirkin  
*Angew. Chem. Int. Ed.* **2006**, *45*, 7220–7223.

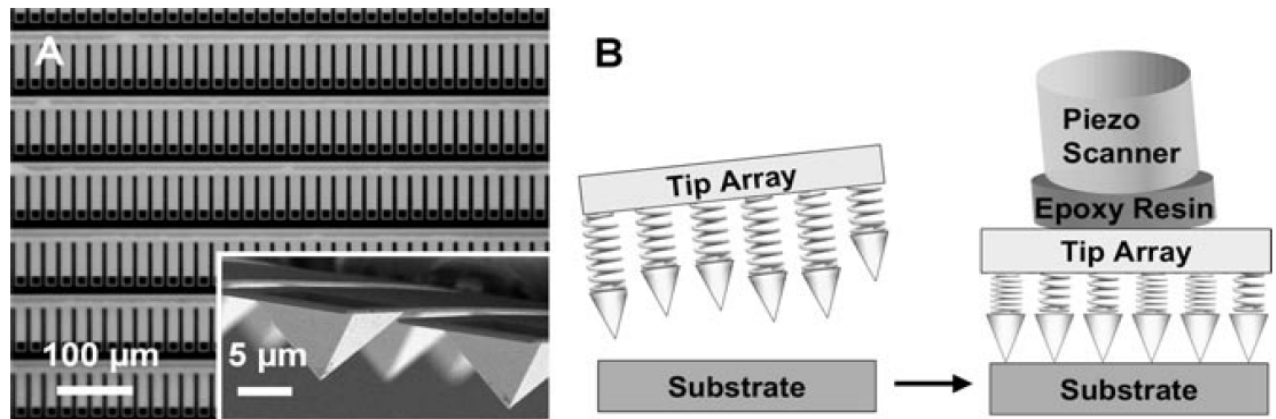
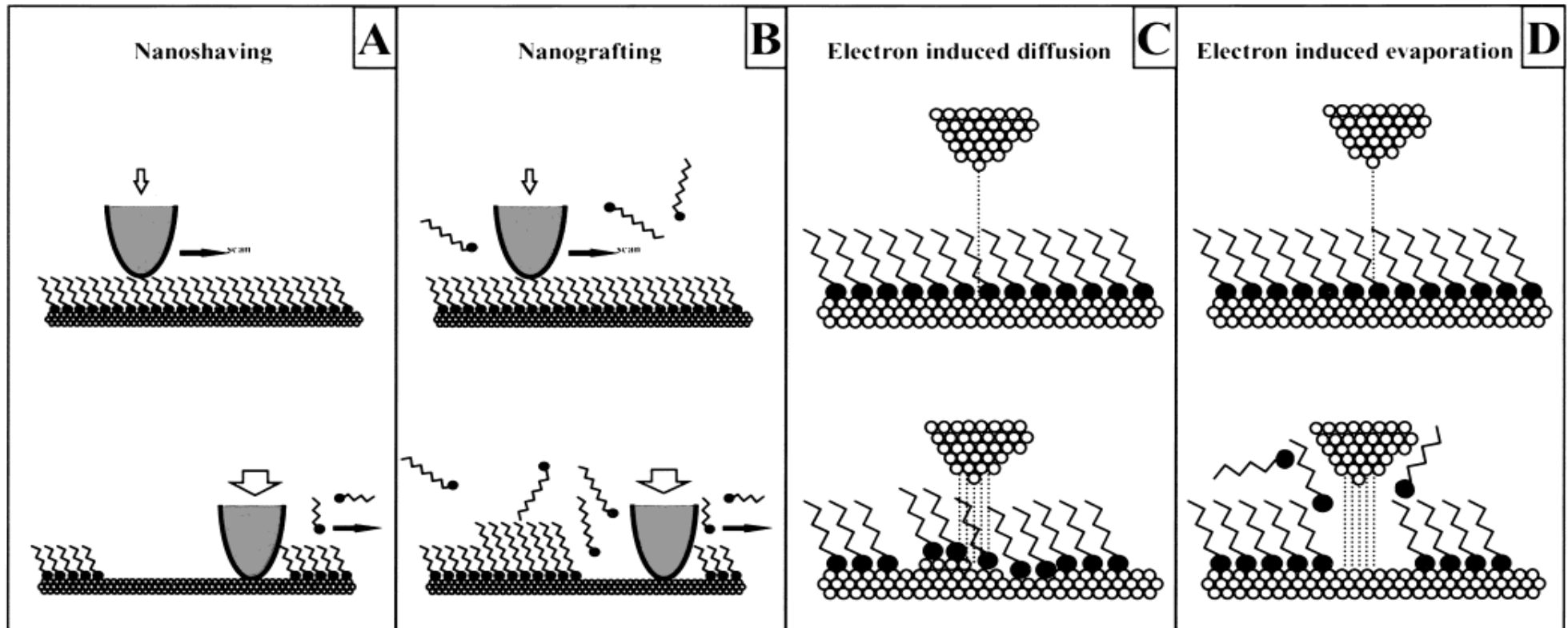


**Figure 1.** A) Optical micrograph of part of the 2D array of cantilevers used for patterning. Inset: SEM image of the cantilever arrays at a different viewing angle. B) Schematic of the gravity-driven alignment method used for massively parallel DPN with a 2D cantilever array. Each pen was brought into contact with the substrate under the weight of the whole pen array. Subsequently, the exact position of the pen array was locked to the AFM scanner head by an epoxy resin.

## Nanofabrication of Self-Assembled Monolayers Using Scanning Probe Lithography



Schematic diagrams of four basic manipulation mechanisms using AFM (A and B) and STM (C and D). The imaging and fabrication modes are depicted in the top and bottom rows, respectively.

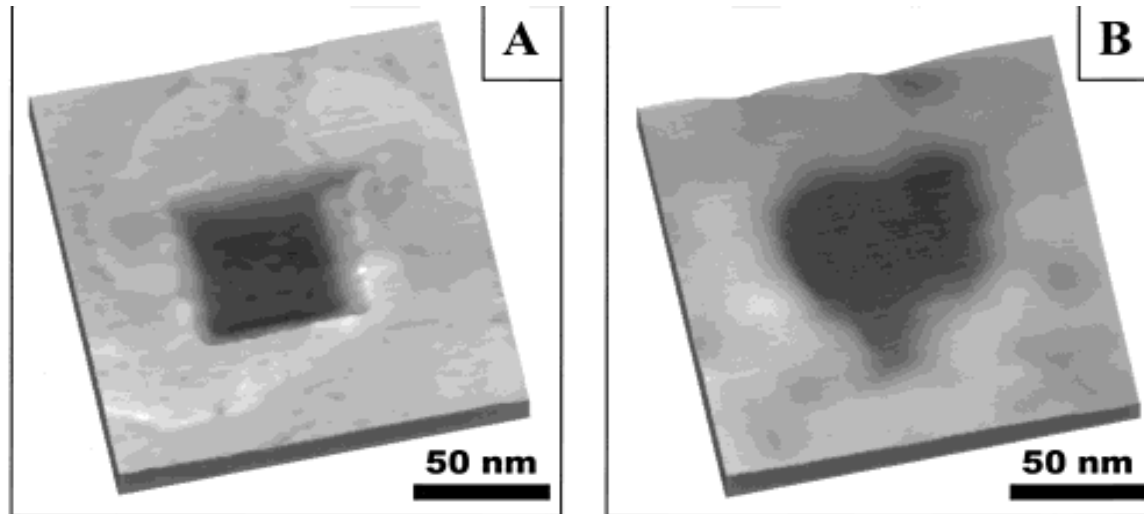


**FIGURE 3.** (A) 160 × 160 nm<sup>2</sup> topographic images of C18S/Au(111) with the thiols shaved away from the central 50 × 50 nm<sup>2</sup> square. (B) 160 × 160 nm<sup>2</sup> topographic images of OTE/mica containing a heart-shaped pattern produced using nanoshaving.

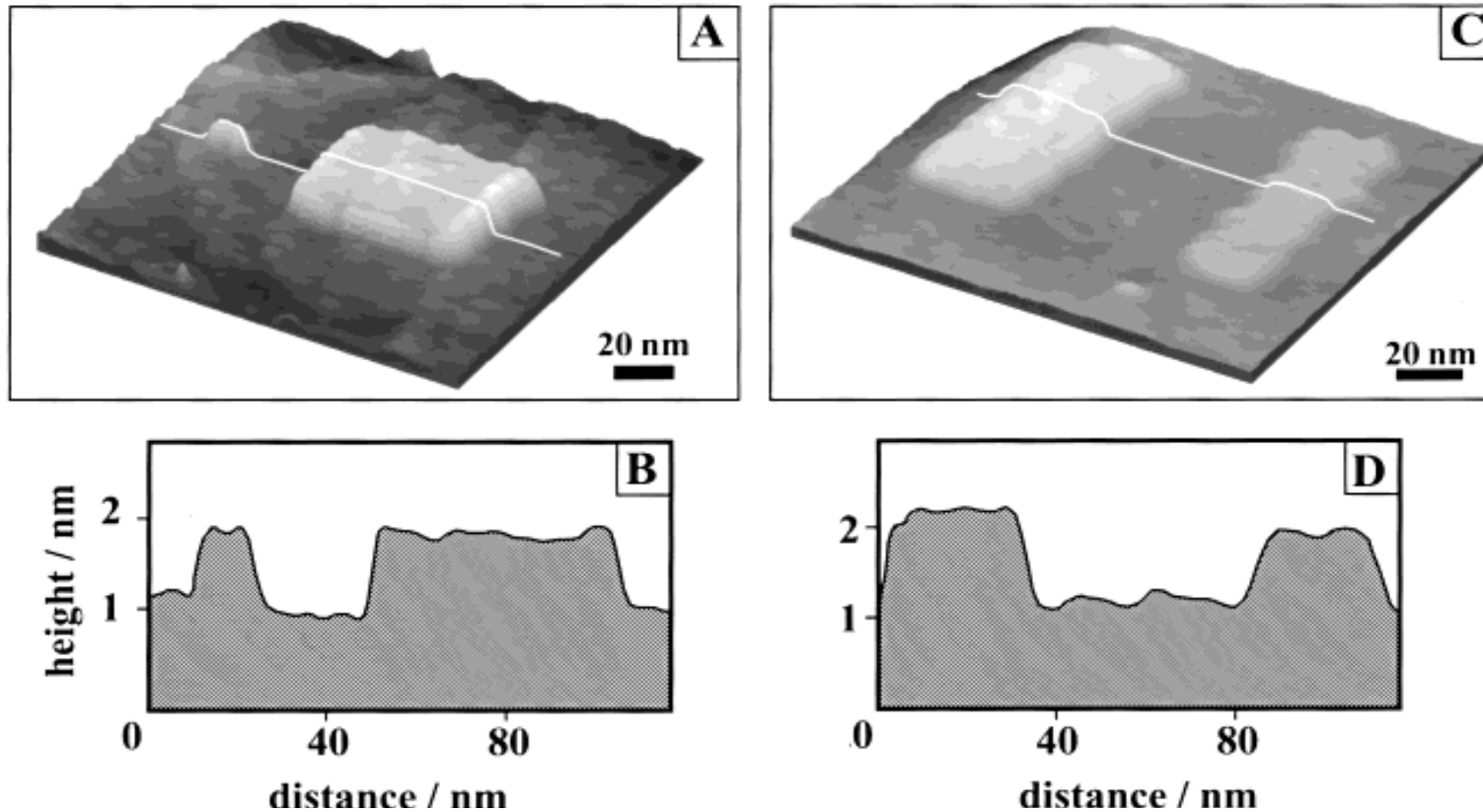


**FIGURE 4.** (A) Fabrication of two C18S nanoislands ( $3 \times 5$  and  $50 \times 50$  nm<sup>2</sup>) in the matrix of a C10S monolayer using nanografting. As shown in the cursor profile (B), the C18S islands are  $8.8 \text{ \AA}$  higher than the surrounding C10S monolayer, consistent with the theoretical value for crystalline-phase SAMs. (C) Fabrication of multicomponent patterns using nanografting. The dimensions of the C22S (left) and C18S (right) islands are  $30 \times 60$  and  $20 \times 60$  nm<sup>2</sup>, respectively. (D) The corresponding cursor profile shows that the C18S and C22S islands are  $7.5 \pm 1.0$  and  $12.0 \pm 1.5 \text{ \AA}$  taller than the C10S/Au matrix monolayer, respectively.

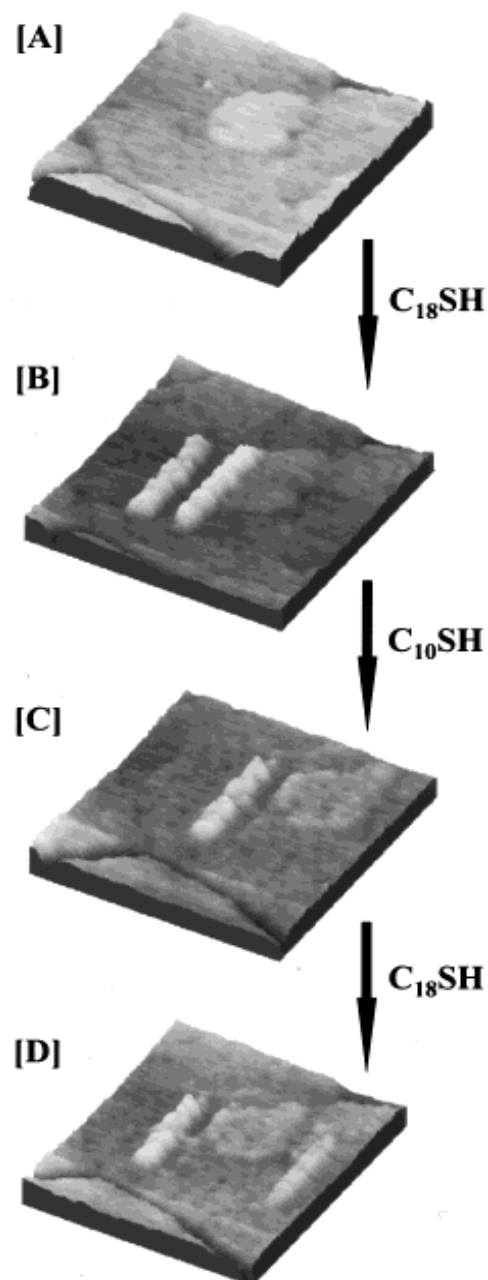


**FIGURE 5.** In situ modification of the grafted nanostructures. (A) AFM image of the matrix C10S SAM before fabrication. The bright area that is 30 nm in diameter and 0.25 nm higher than the rest of the surface is due to a single atomic step of Au(111) covered by the C10S SAM. (B) After fabrication of two parallel C18S nanolines with dimensions of 10 50 nm<sup>2</sup> and a separation of 20 nm. (C) Erasure of the right line by scanning its area under a high imaging force in a C10SH solution. (D) Refabrication of the second line by scanning under a high imaging force in C18SH solution. The interline spacing was increased to 65 nm. The spatial precision for this fabrication is 2 nm.

## Nanografting

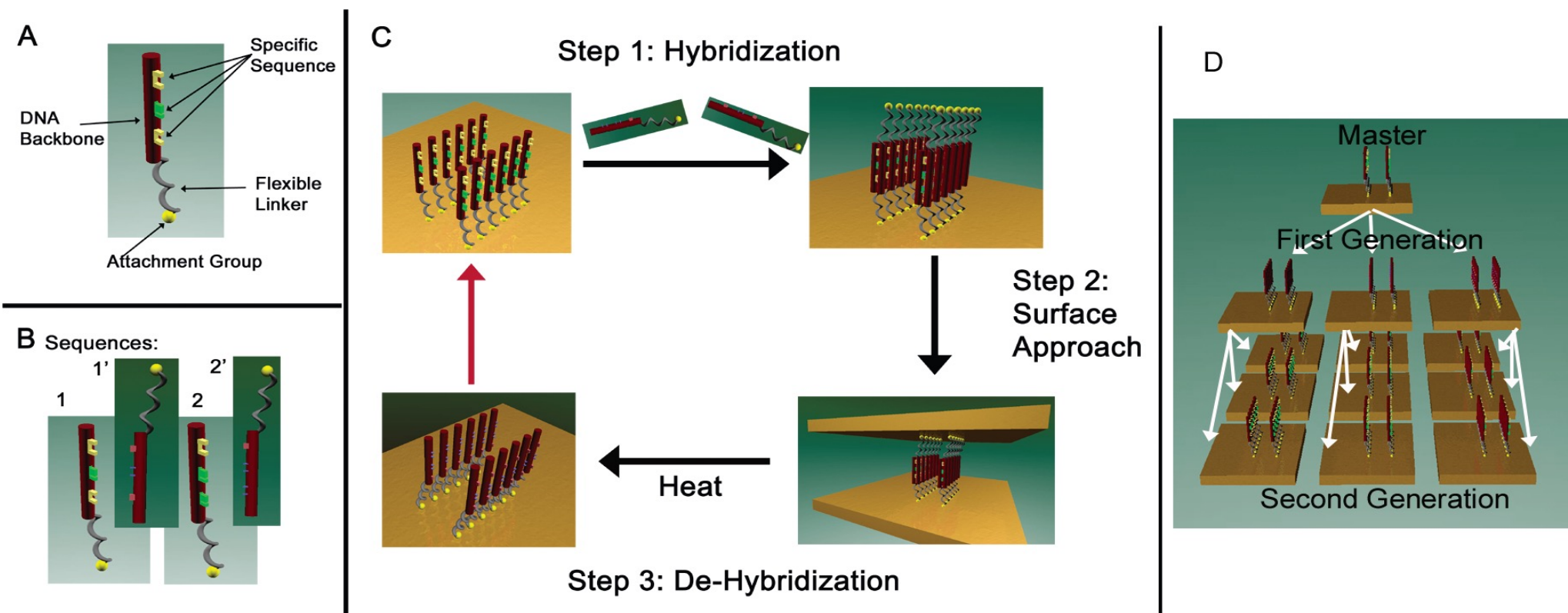
### Advantage:

- surface can be imaged and patterned with different molecules by the same tip under exactly the same situation. It is thus possible to compare molecular properties in a differential way, minimizing tip-induced and other environmental effects.
- By using lateral force microscopy and the conducting-tip AFM, electron transfer and friction properties of the molecules can be correlated with topography information.



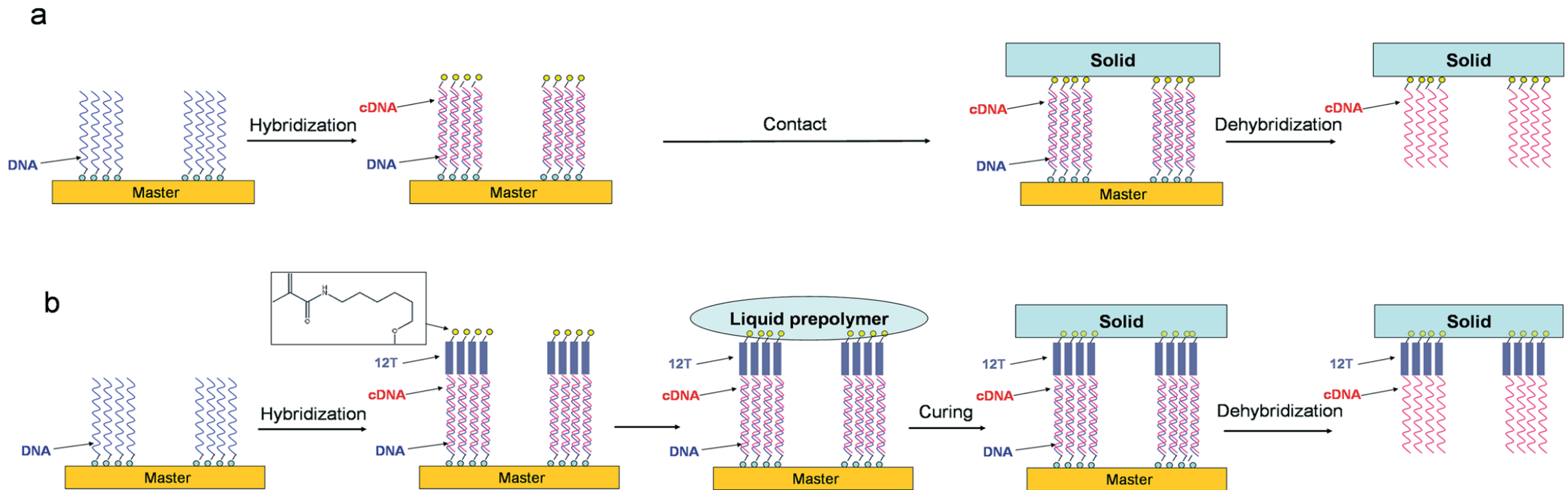
## Supramolecular Nanostamping: Using DNA as Movable Type

## SuNS



A. Yu, T. A. Savas, G. S. Taylor, A. Guiseppe-Elie, H. I. Smith, F. Stellacci *Nano Lett.*, **2005**, 5, 1061-1064.

## Contact Printing Beyond Surface Roughness: Liquid Supramolecular Nanostamping

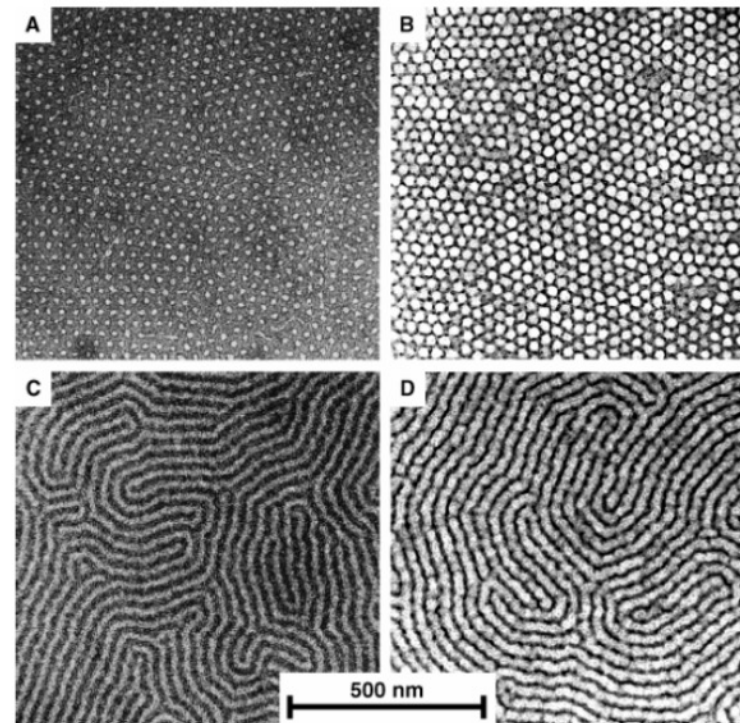


Schematic drawing of (a) SuNS' and (b) LiSuNS' process steps. The use of a viscous liquid precursor to a solid substrate introduces one more step in LiSuNS, but completely removes the issues involved in the contact of two solid surfaces. Note that LiSuNS is a simpler technique because it does not need any contact instrumentation and because it does not require any secondary surface treatment.

A. A. Yu, F. Stellacci *Adv. Mater.* **2007**, *19*, 4338–4342.

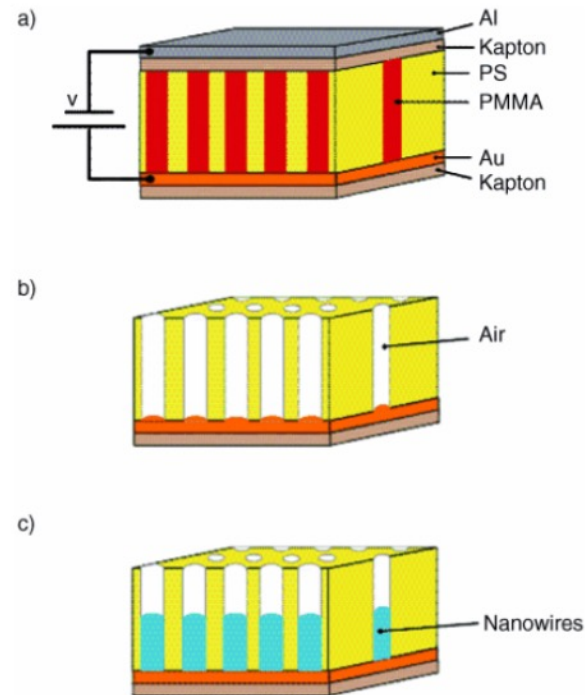
**TEM micrographs of polystyrene-polybutadiene diblock copolymer film masks (a,c) and lithographically patterned silicon nitride (b,d).**

(C. Harrison, Science)

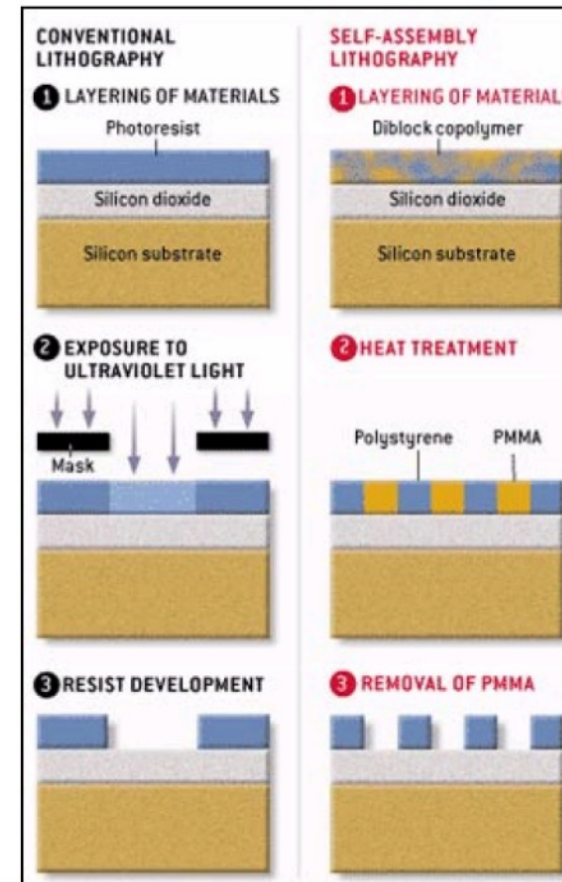


**Nanowire-array formation. a) An asymmetric diblock copolymer is annealed above the glass transition temperature of the copolymer between two electrodes under an applied electric field. b) After removal of the minor component, a nanoporous film is formed. c) Nanowires formed by electrodeposition in 20 nm pores.**

(from M.T. Tuominen, Science)

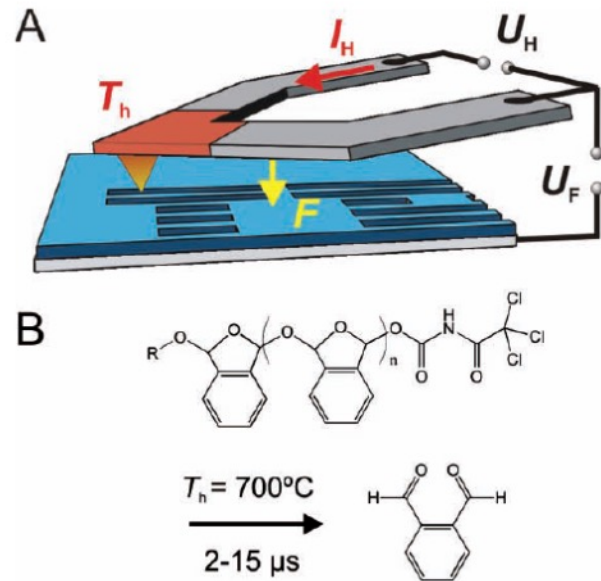


Self-assembly patterning occurs when a diblock copolymer is heated, thereby separating the two polymers in the material into defined areas before the PMMA is etched away. The template of cylindrical holes is transferred into the silicon dioxide before the holes are filled with nanocrystalline silicon used to store data (20 nm size).

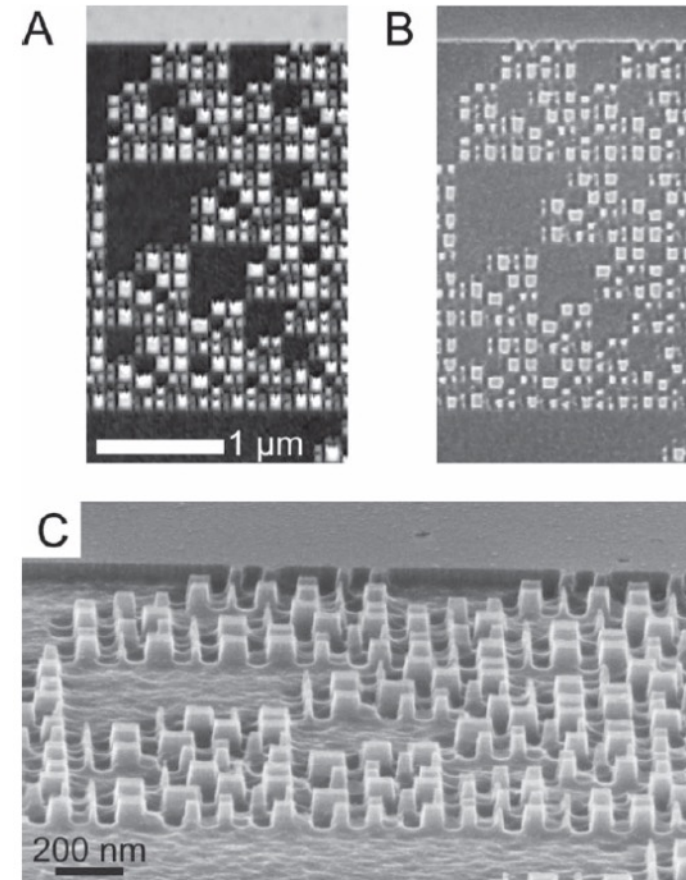


## Probe-Based 3-D Nanolithography Using Self-Amplified Depolymerization Polymers

A. W. Knoll, D. Pires, O. Coulembier, P. Dubois, J. L. Hedrick, J. Frommer, U. Duerig *Adv. Mater.* **2010**, 22, 3361–3365.



A) Schematic of the patterning method. The AFM-style cantilever comprises integrated heaters for heating the tip and for sensing the topography (not shown). The tip rests  $\sim 300$  nm above the surface if no voltages are applied. To pattern a pixel, short voltage pulses  $U_H$  and  $U_F$  are applied to heat the tip and to pull the tip into contact by electrostatic means, respectively. B) Structure of the polyphthalaldehyde polymer used in this study. At typical patterning parameters, heater temperature of  $T_H = 700$  °C and pulse durations of 2–14  $\mu$ s, the polymer is converted into its monomer constituents by self-amplified depolymerization.



A) AFM topographical image of a pattern created using a heater temperature of 700 °C and a force pulse duration of 2  $\mu$ s. The patterning depth amounts to 16 nm in a 50 nm thick polyphthalaldehyde film. B) Scanning electron microscopy image of the same area after reactive ion etching (RIE) into the silicon substrate. C) Tilted view (45°) of the same area. The height of the structures is  $\sim 90$  nm, corresponding to a depth amplification by a factor of 6. The thin pillars are  $\sim 30$  nm wide, whereas the grooves between the structures are  $\sim 50$  nm wide.

## Nanoscale Three-Dimensional Patterning of Molecular Resists by Scanning Probes

D. Pires, J. L. Hedrick, A. De Silva, J. Frommer, B. Gotsmann, H. Wolf, M. Despont, U. Duerig, A. W. Knoll *Science*, **2010**, 328, 732.

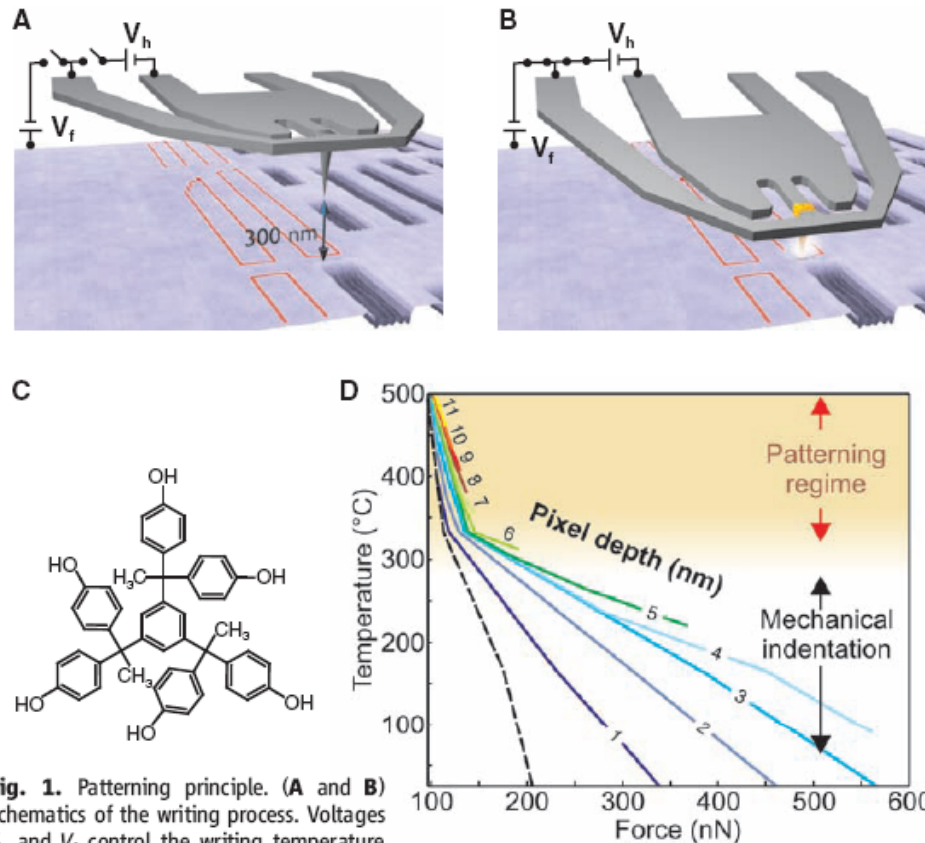


**Fig. 1.** Patterning principle. **(A and B)** Schematics of the writing process. Voltages  $V_h$  and  $V_f$  control the writing temperature and the electrostatic force, respectively. If no voltage is applied (A), the tip rests 300 nm above the surface. A pixel in the programmed bitmap (red outline) is written by simultaneously applying a force and temperature pulse for several microseconds. The force pulse pulls the tip into contact while the heat pulse heats the tip and triggers the patterning process. **(C)** Molecular structure of the phenolic compound used as resist. **(D)** Equi-depth lines of the pixels created in the resist upon single exposure events as a function of applied temperature and force. The dashed line indicates the writing threshold, determined by extrapolation to zero depth. Two regimes are separated by a threshold temperature of  $\sim 330^\circ\text{C}$ . Below the threshold, the resist is mechanically deformed; above the threshold, it is efficiently removed.

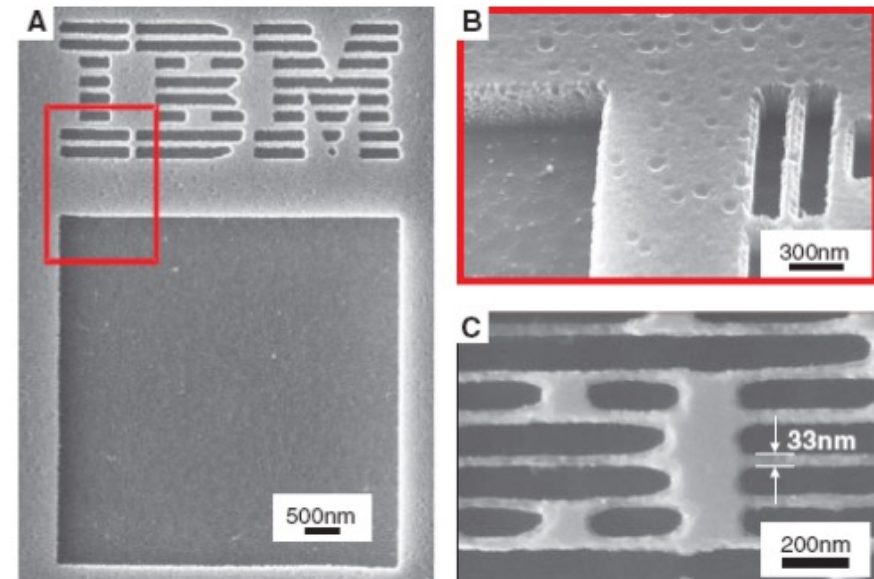


**Fig. 3.** Pattern transfer into silicon. **(A)** SEM image of the pattern shown in Fig. 2 transferred 400 nm deep into silicon. **(B)** Tilted view of the structure indicated by the red box in (A). **(C)** Zoom into a similar structure as shown in (A) but written at half the pixel pitch. The smallest lines fabricated in silicon had a width of  $\sim 30$  nm.